US 20130009014A1

(19) **United States**

(12) **Patent Application Publication**

BORDETSKY et al.

(10) **Pub. No.: US 2013/0009014 A1**

(43) **Pub. Date: Jan. 10, 2013**

(54) **INSTANTANEOUS WIRELESS NETWORK ESTABLISHED BY SIMULTANEOUSLY DESCENDING PARAFOILS**

(76) Inventors: **Alex BORDETSKY**, Carmel, CA (US); **Oleg Yakimenko**, Seaside, CA (US); **Eugene Bourakov**, Carmel, CA (US)

(21) Appl. No.: **13/083,511**

(22) Filed: **Apr. 8, 2011**

Related U.S. Application Data

(60) Provisional application No. 61/324,222, filed on Apr. 14, 2010, provisional application No. 61/324,551, filed on Apr. 15, 2010, provisional application No. 61/323,792, filed on Apr. 13, 2010, provisional application No. 61/323,750, filed on Apr. 13, 2010, provisional application No. 61/323,675, filed on Apr. 13, 2010.

Publication Classification

(51) **Int. Cl.**

G05D 1/00	(2006.01)
H04W 4/00	(2009.01)
B64C 13/20	(2006.01)

(52) **U.S. Cl.** **244/189**; 370/328

(57) **ABSTRACT**

A method is described that involves establishing a wireless network between a wireless access node of an existing network and a remote location by wirelessly linking a plurality of electronic processing circuits each transported by a respective parafoil. The wirelessly linked processing circuits are to route packets from the wireless access node to the remote location.

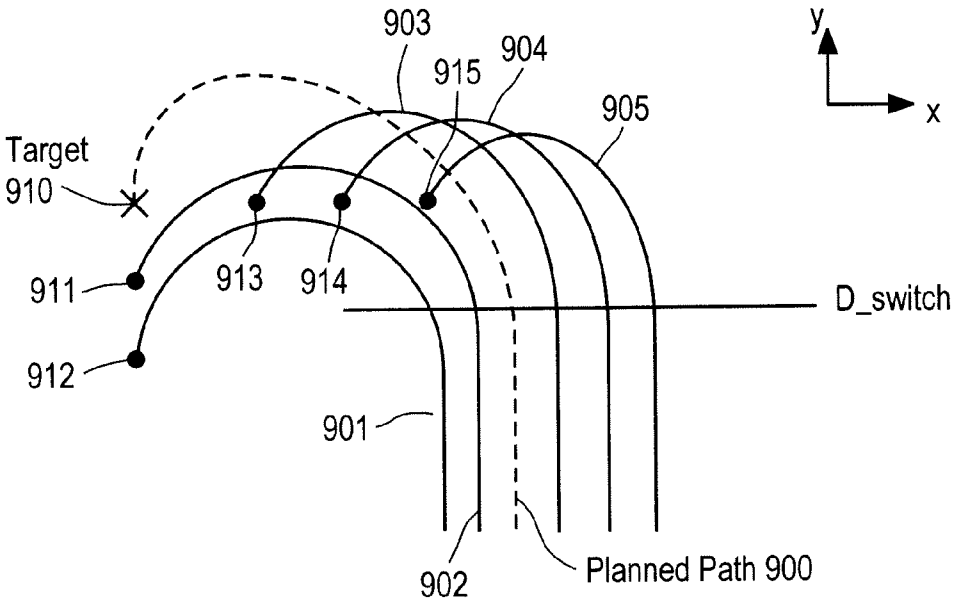

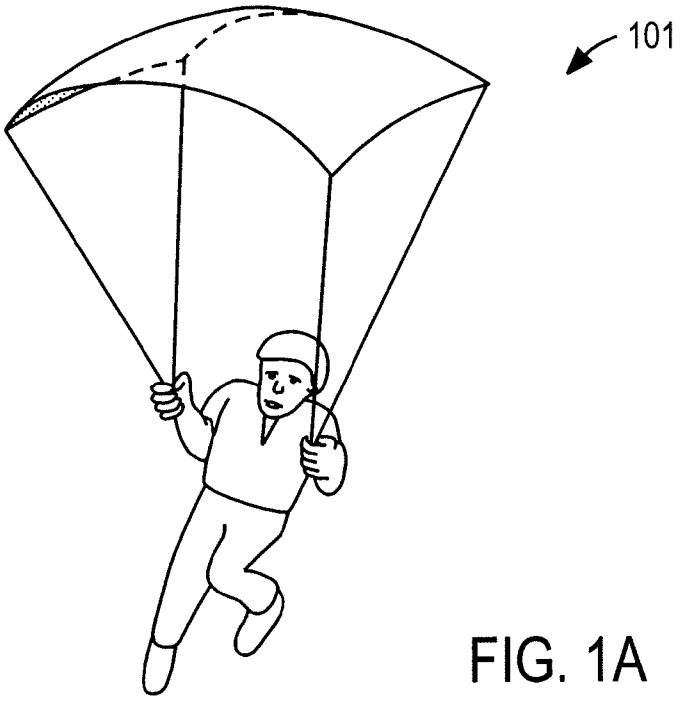

FIG. 1A

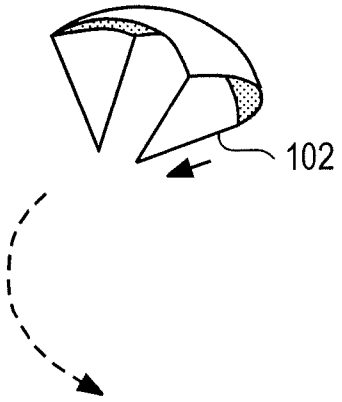

FIG. 1B

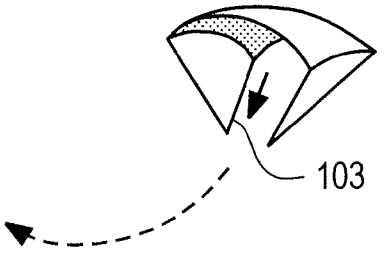

FIG. 1C

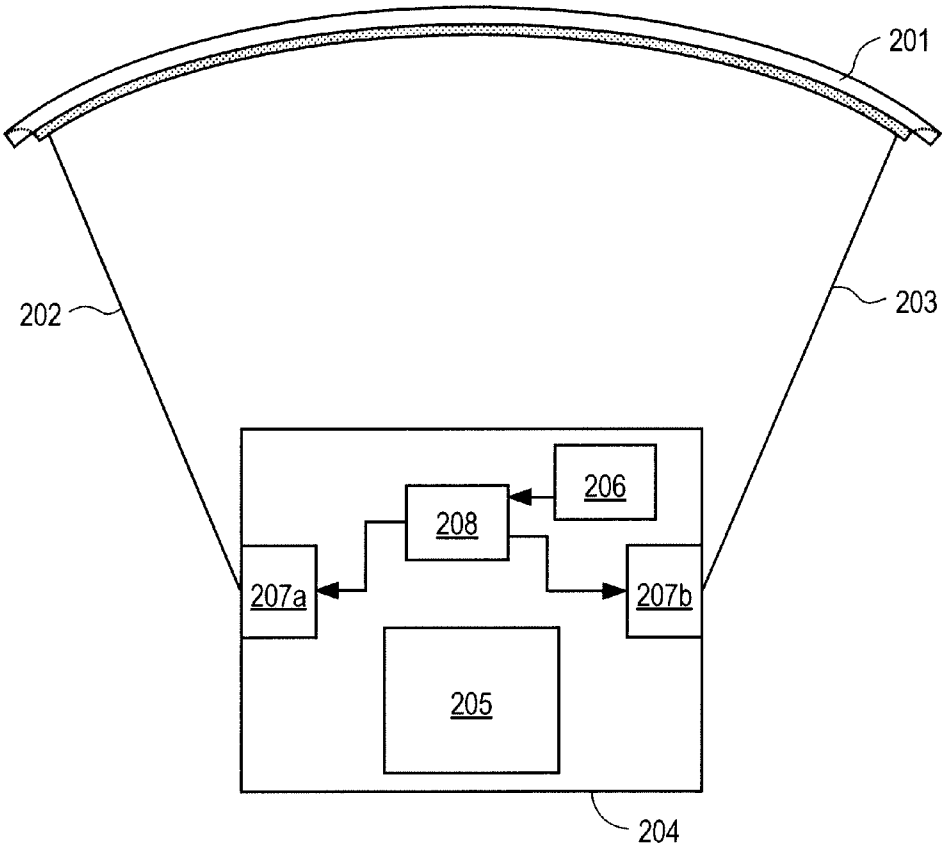

FIG. 2

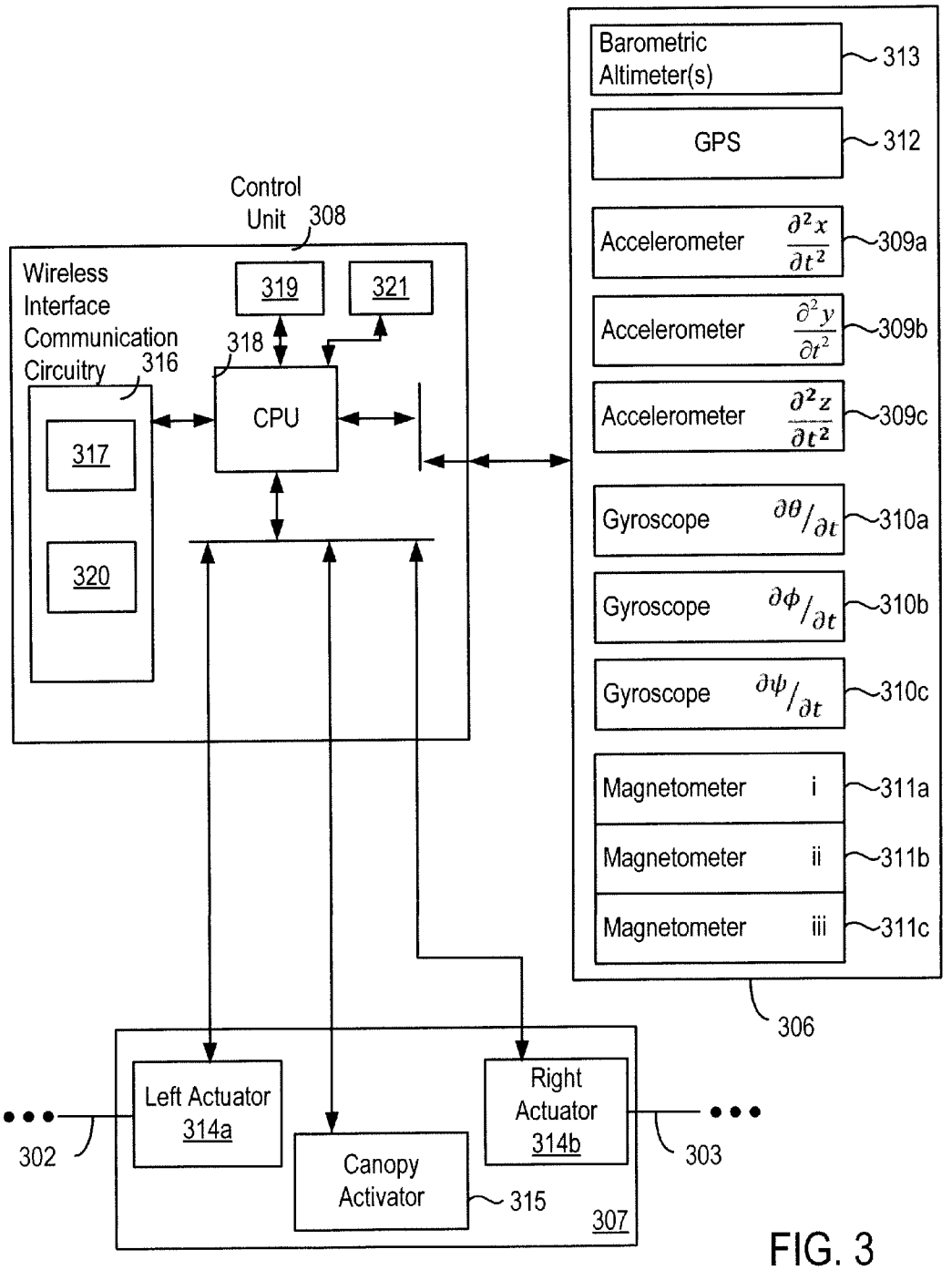
Barometric Altimeter(s)
313
GPS
312
Accelerometer $\frac{\partial^2 x}{\partial t^2}$
309a
Accelerometer $\frac{\partial^2 y}{\partial t^2}$
309b
Accelerometer $\frac{\partial^2 z}{\partial t^2}$
309c
Gyroscope $\partial\theta/\partial t$
310a
Gyroscope $\partial\phi/\partial t$
310b
Gyroscope $\partial\psi/\partial t$
310c
Magnetometer i
311a
Magnetometer ii
311b
Magnetometer iii
311c
306
Control Unit 308
Wireless Interface Communication Circuitry 316
319
321
318
CPU
317
320
Left Actuator 314a
Right Actuator 314b
Canopy Activator
315
307
302
303

FIG. 3

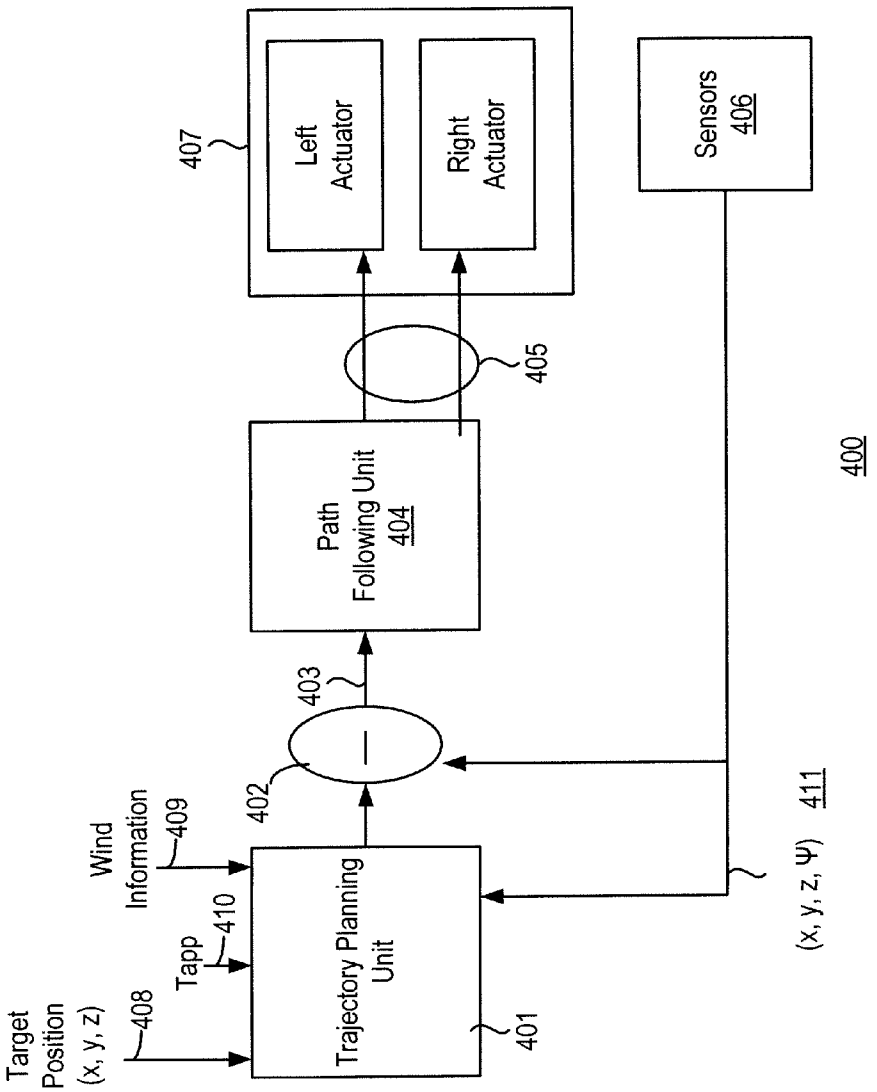
Target Position (x, y, z)
408
Tapp
410
Wind Information
409
Trajectory Planning Unit
401
402
403
Path Following Unit 404
405
407
Left Actuator
Right Actuator
Sensors 406
(x, y, z, Ψ) 411
400

FIG. 4

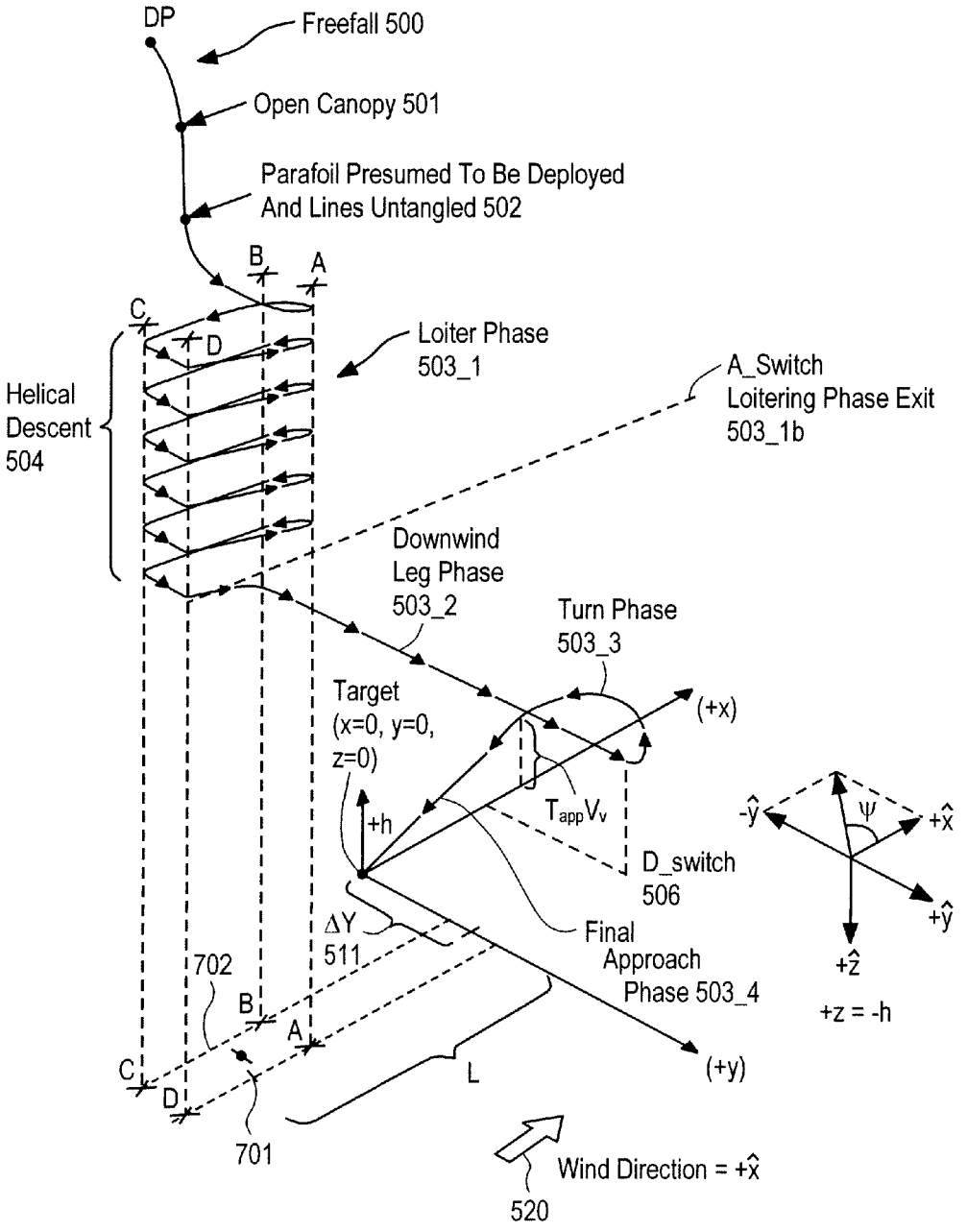
DP
Freefall 500
Open Canopy 501
Parafoil Presumed To Be Deployed
And Lines Untangled 502
B
A
C
D
Loiter Phase
503_1
A_Switch
Loitering Phase Exit
503_1b
Helical
Descent
504
Downwind
Leg Phase
503_2
Turn Phase
503_3
Target
(x=0, y=0,
z=0)
(+x)
+h
$T_{app}V_v$
D_switch
506
ΔY
511
Final
Approach
Phase 503_4
702
B
A
C
D
L
(+y)
701
Wind Direction = +x̂
520
-ŷ
ψ
+x̂
+ŷ
+ẑ
+z = -h

FIG. 5

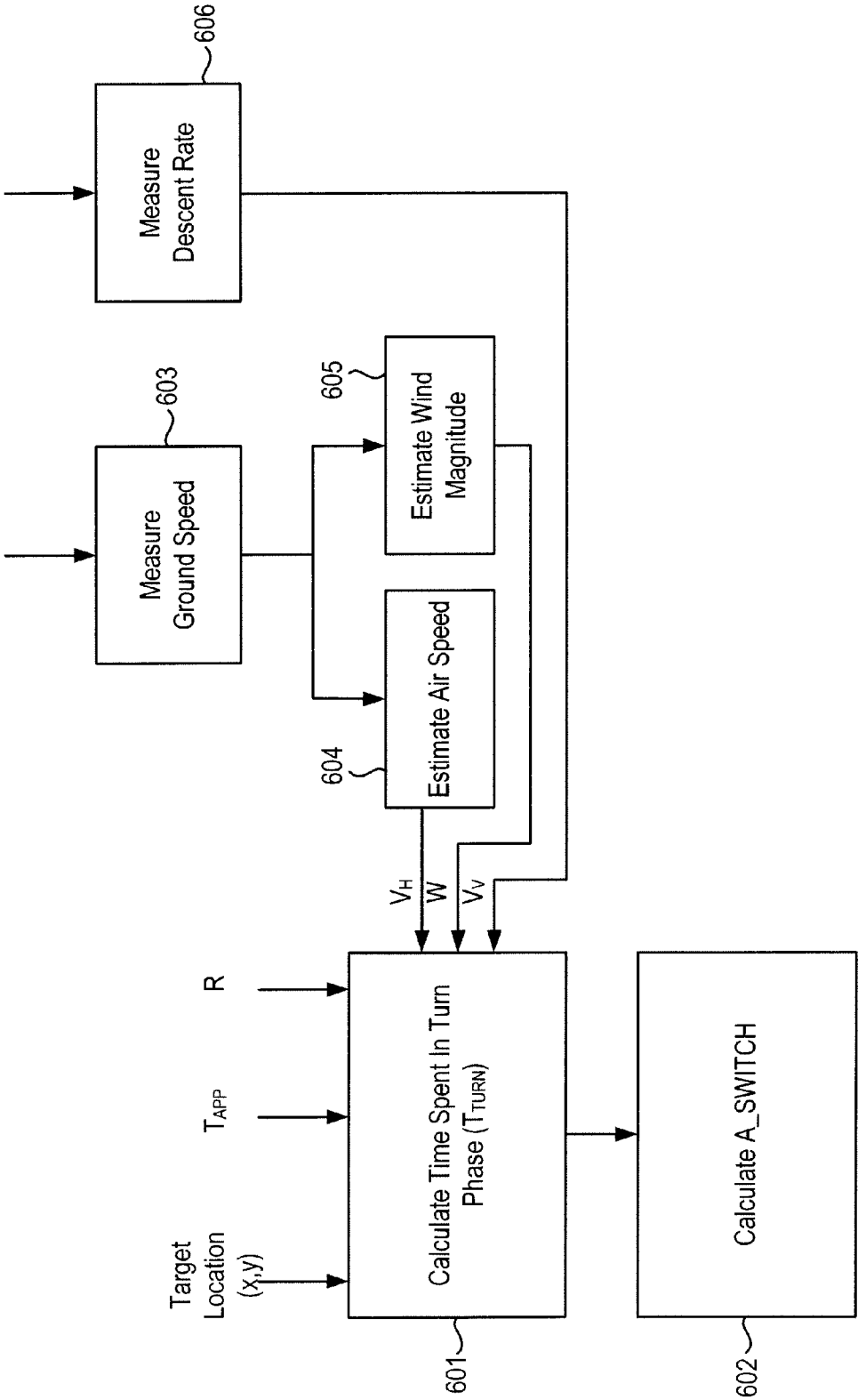
606
Measure Descent Rate
603
Measure Ground Speed
605
Estimate Wind Magnitude
604
Estimate Air Speed
V_H
W
V_V
R
T_{APP}
Target Location (x,y)
Calculate Time Spent In Turn Phase (T_{TURN})
601
Calculate A_SWITCH
602

FIG. 6

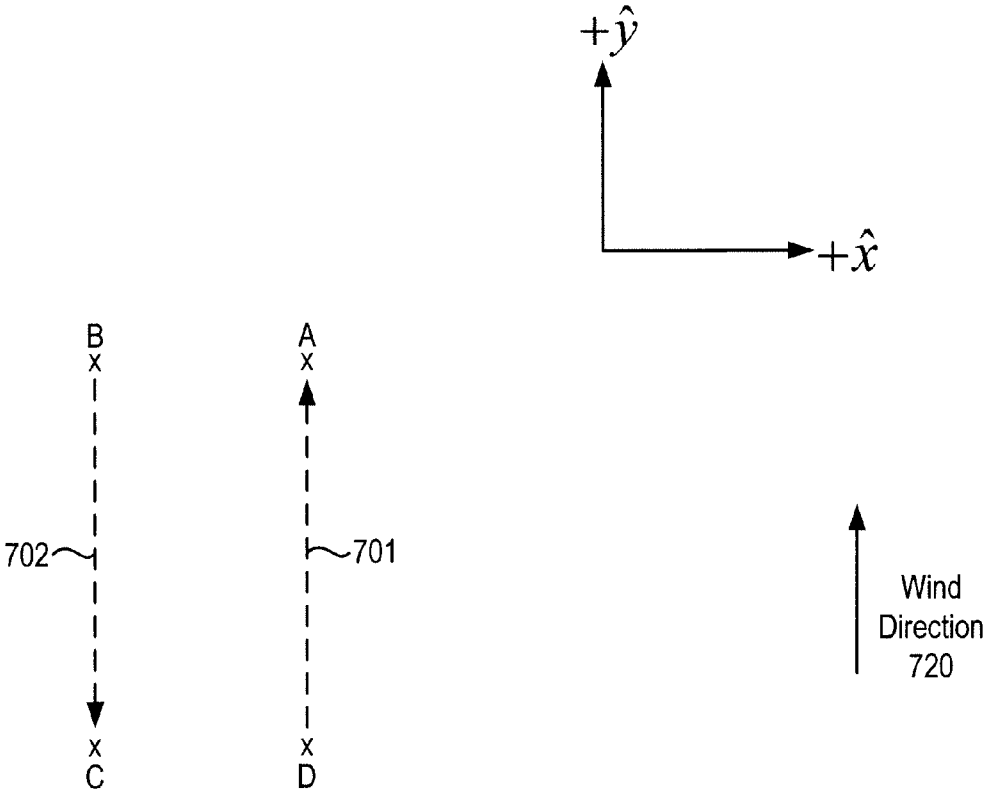

FIG. 7

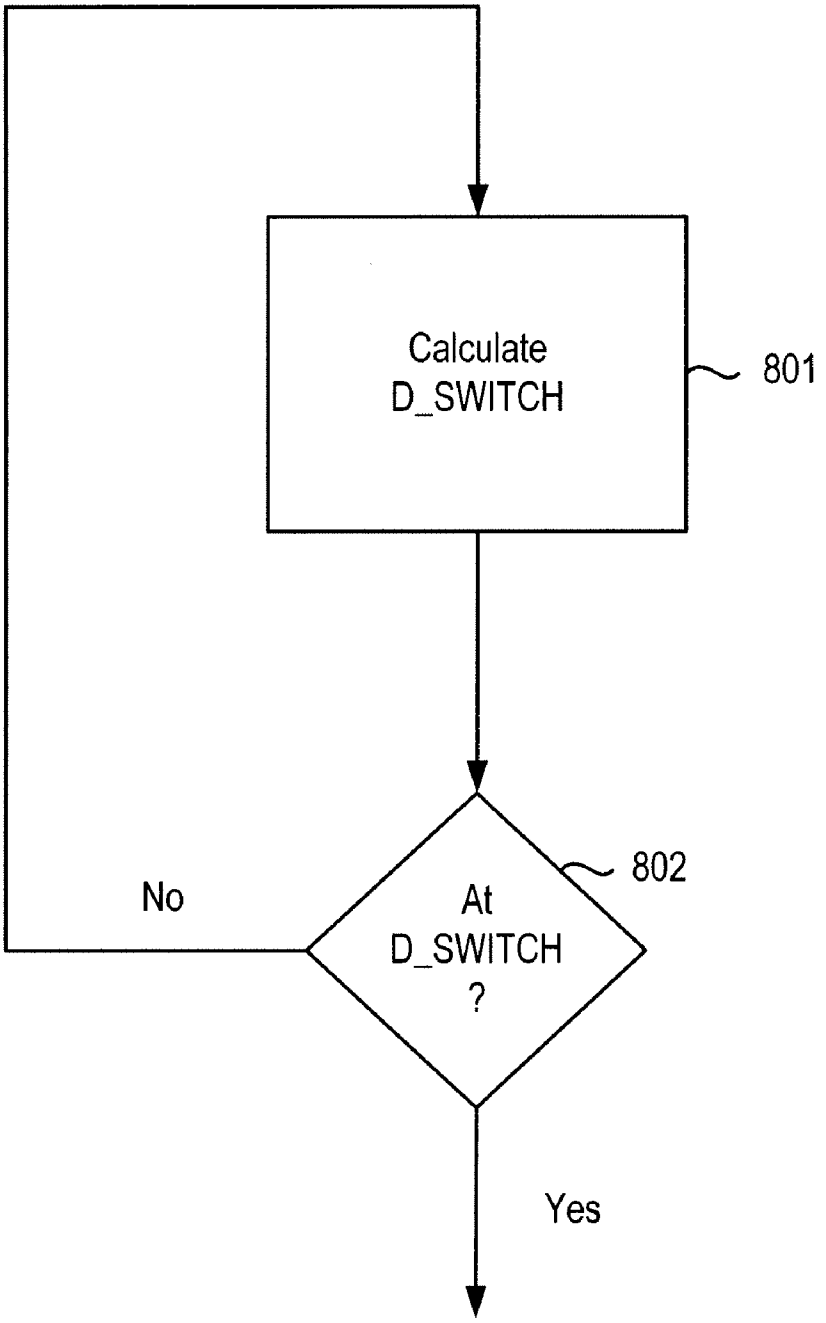

FIG. 8

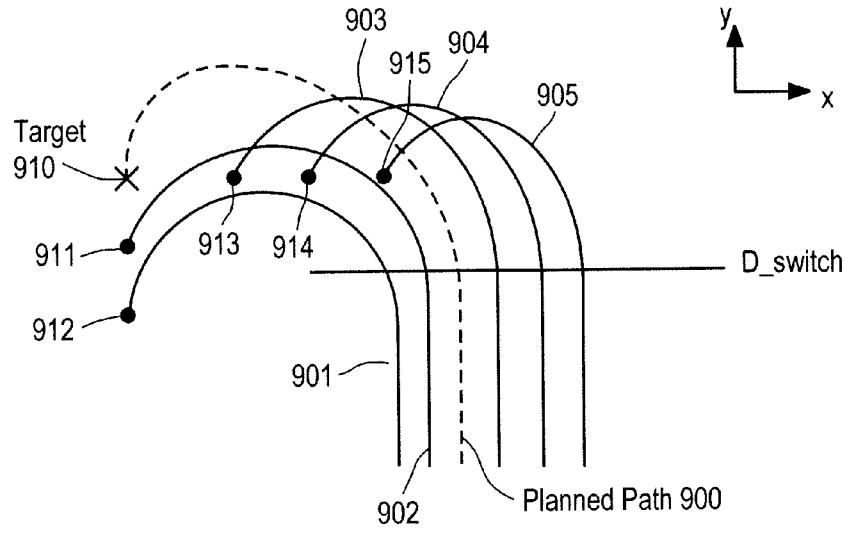
903
915
904
905
y
x
Target
910
911
913
914
912
D_switch
901
902
Planned Path 900

FIG. 9A

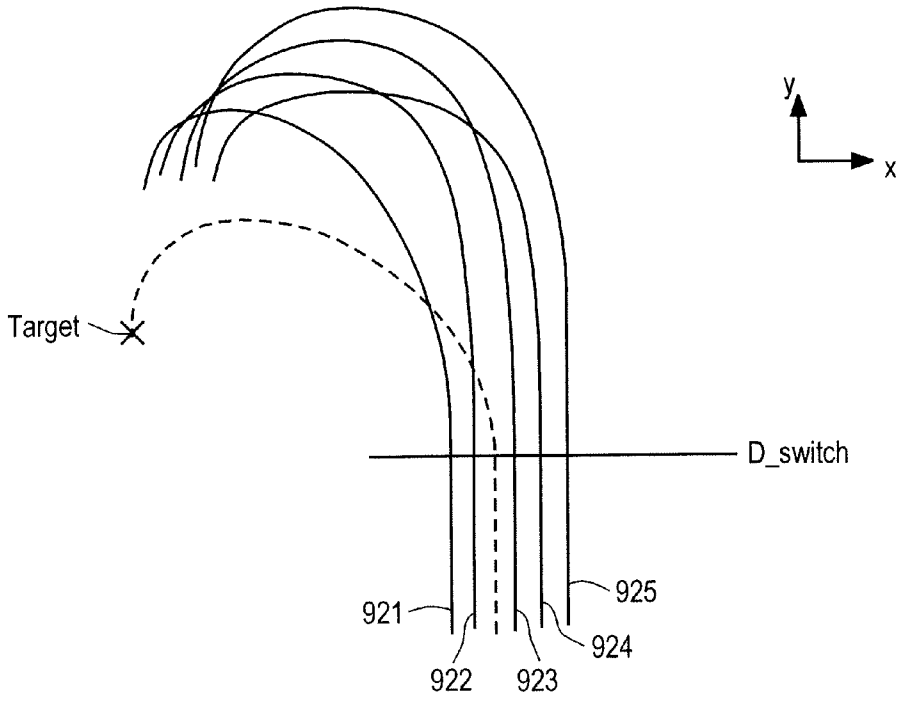
y
x
Target
D_switch
921
922
923
924
925

FIG. 9B

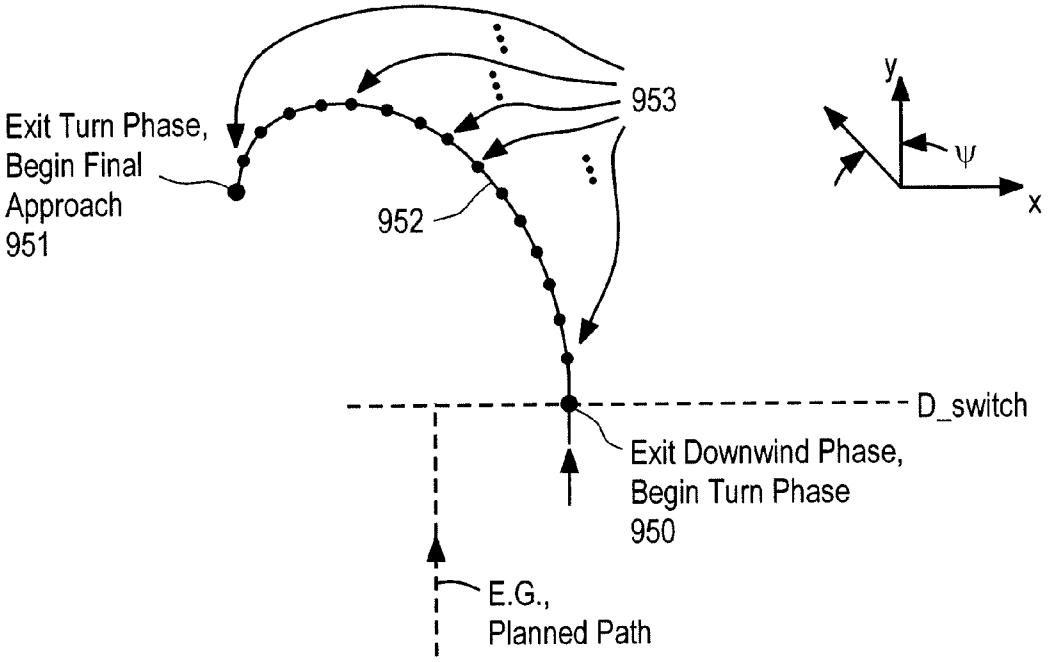
Exit Turn Phase,
Begin Final
Approach
951
953
952
y
ψ
x
D_switch
Exit Downwind Phase,
Begin Turn Phase
950
E.G.,
Planned Path

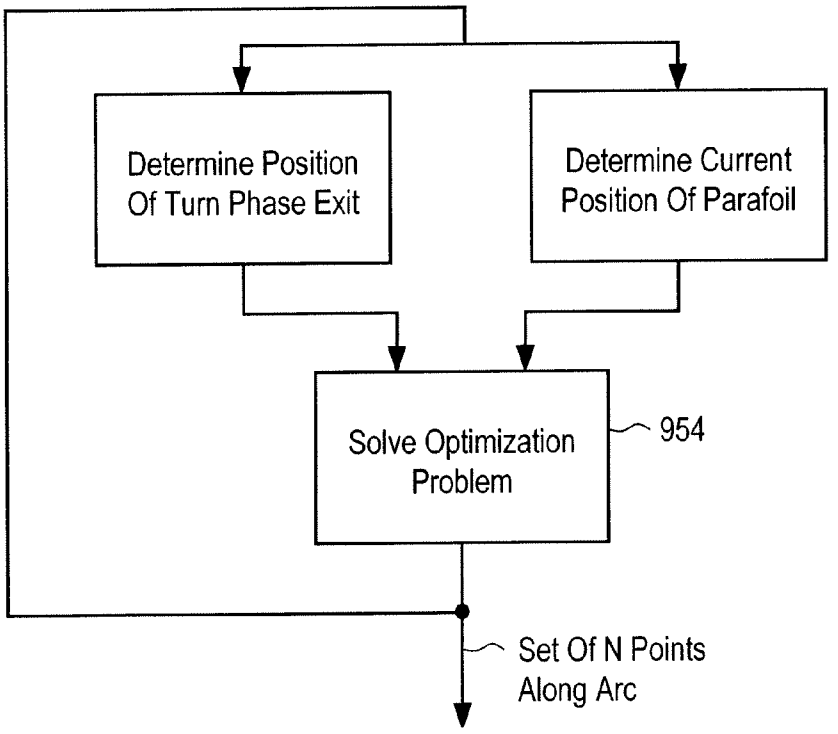
Determine Position
Of Turn Phase Exit
Determine Current
Position Of Parafoil
Solve Optimization
Problem
954
Set Of N Points
Along Arc

FIG. 9C

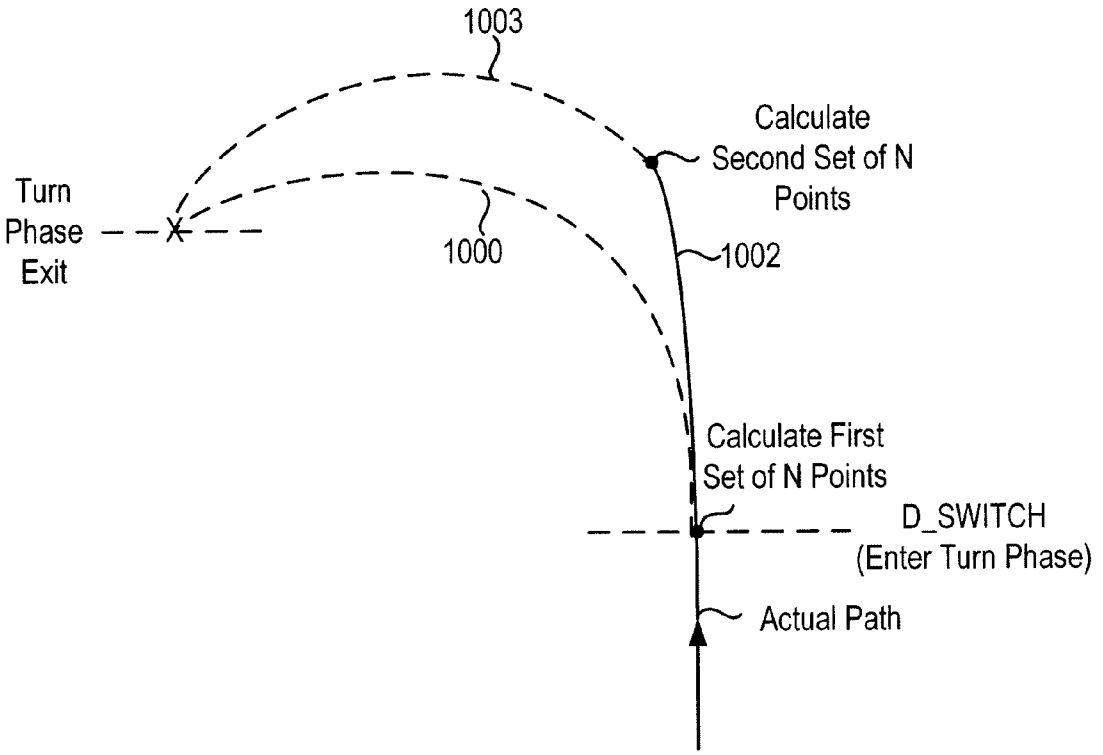
1003
Calculate
Second Set of N
Points
Turn
Phase
Exit
1000
1002
Calculate First
Set of N Points
D_SWITCH
(Enter Turn Phase)
Actual Path

FIG. 10

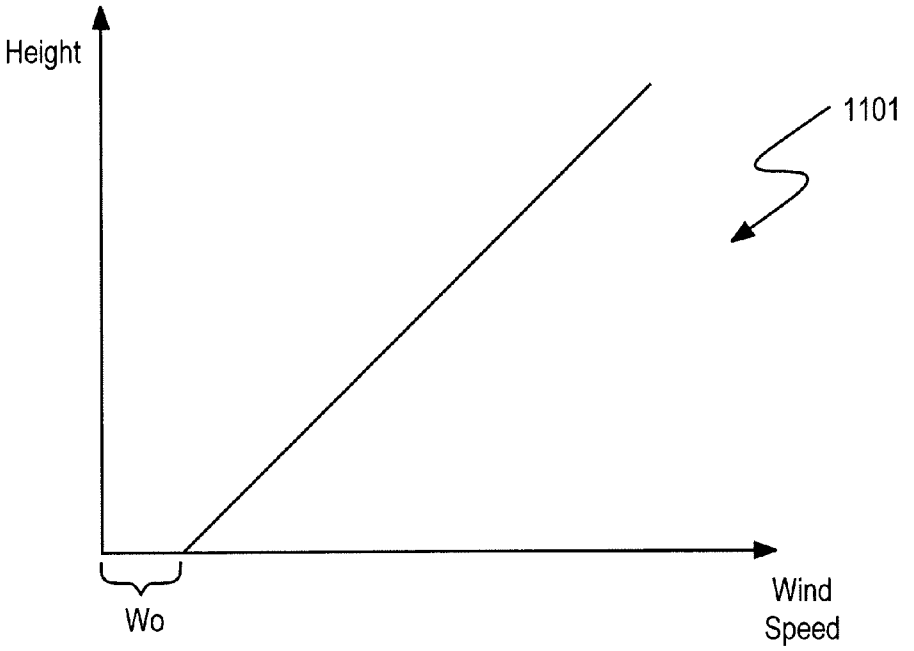

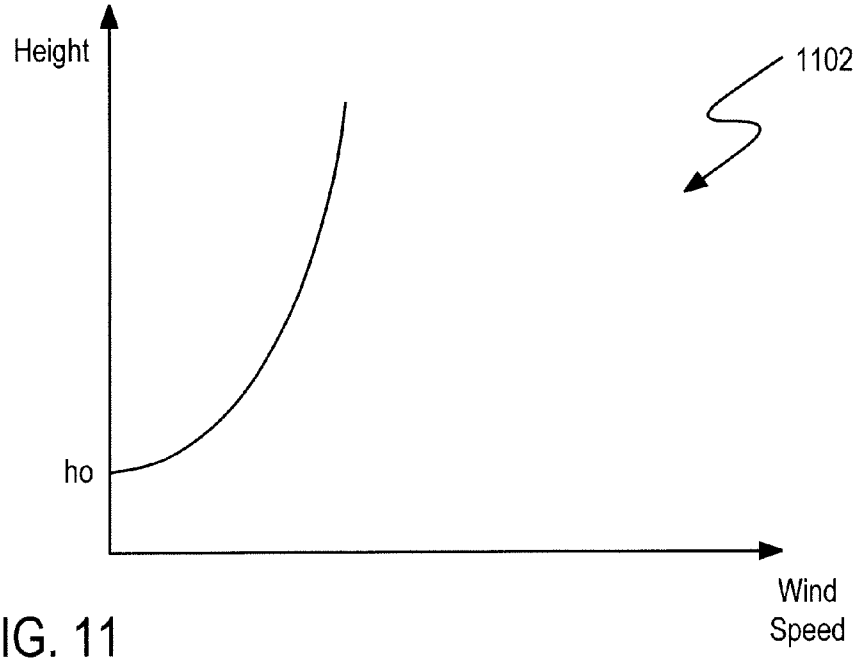

FIG. 11

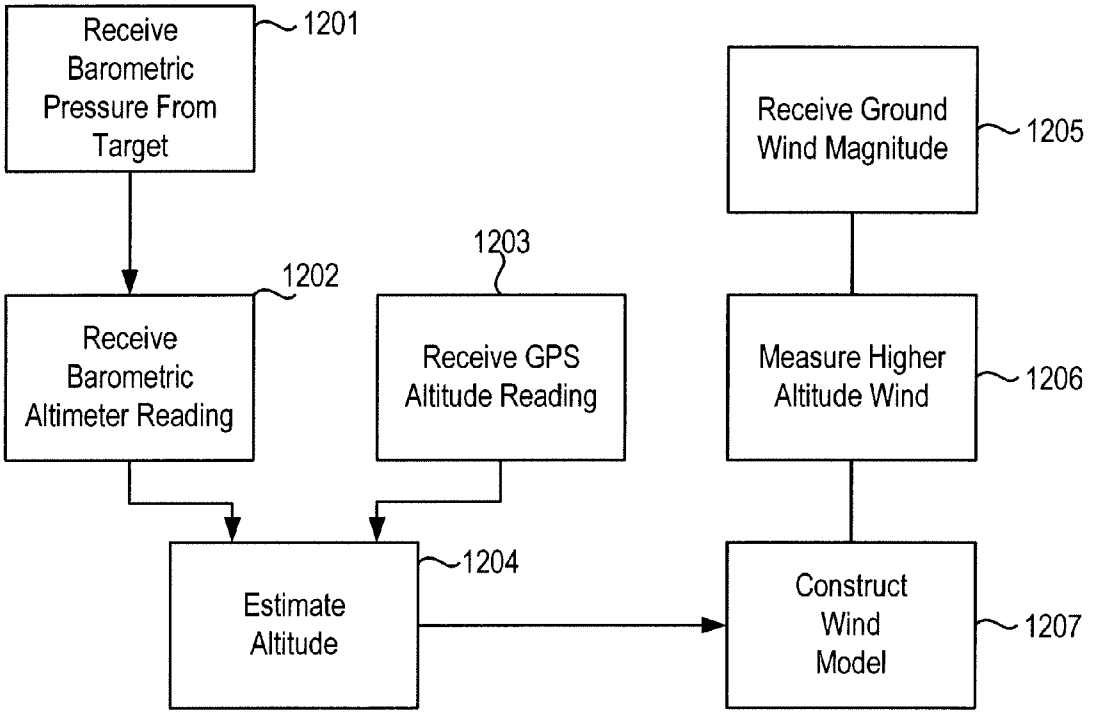
Receive Barometric Pressure From Target
1201
Receive Barometric Altimeter Reading
1202
1203
Receive GPS Altitude Reading
Estimate Altitude
1204
Receive Ground Wind Magnitude
1205
Measure Higher Altitude Wind
1206
Construct Wind Model
1207

FIG.12

FIG. 13A

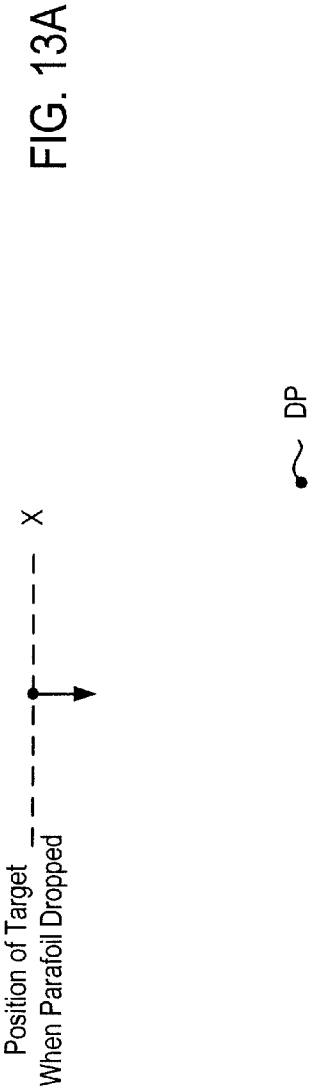

FIG. 13B

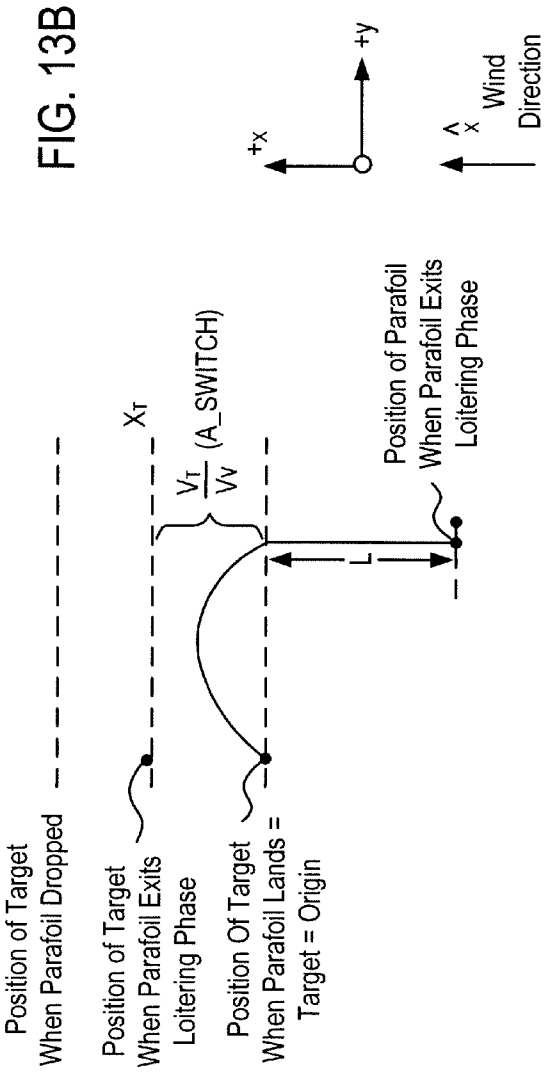

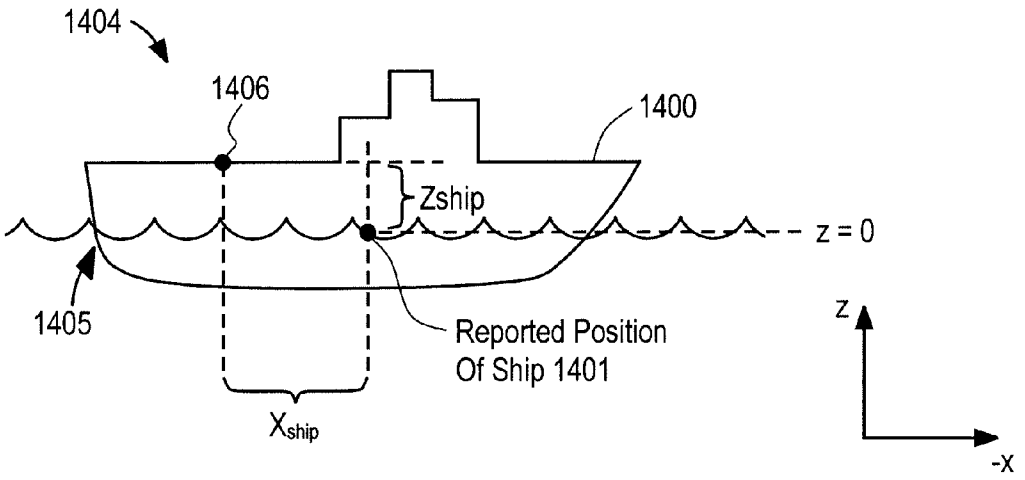

FIG. 14A

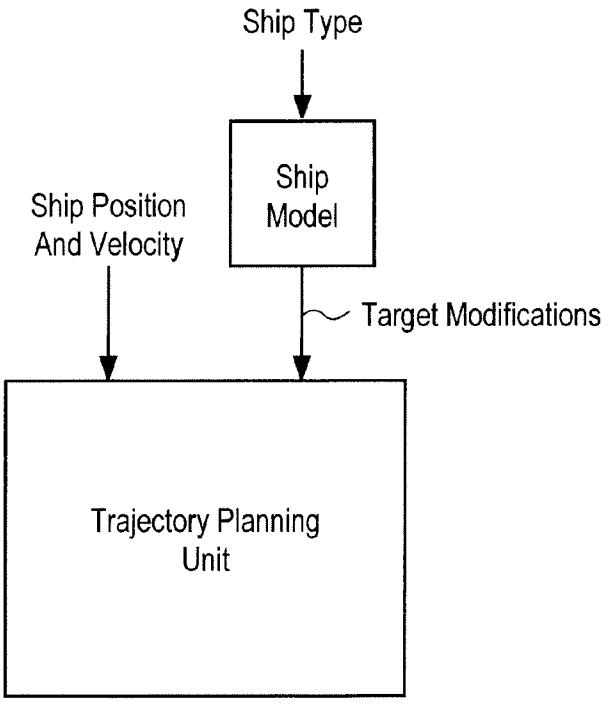

FIG. 14B

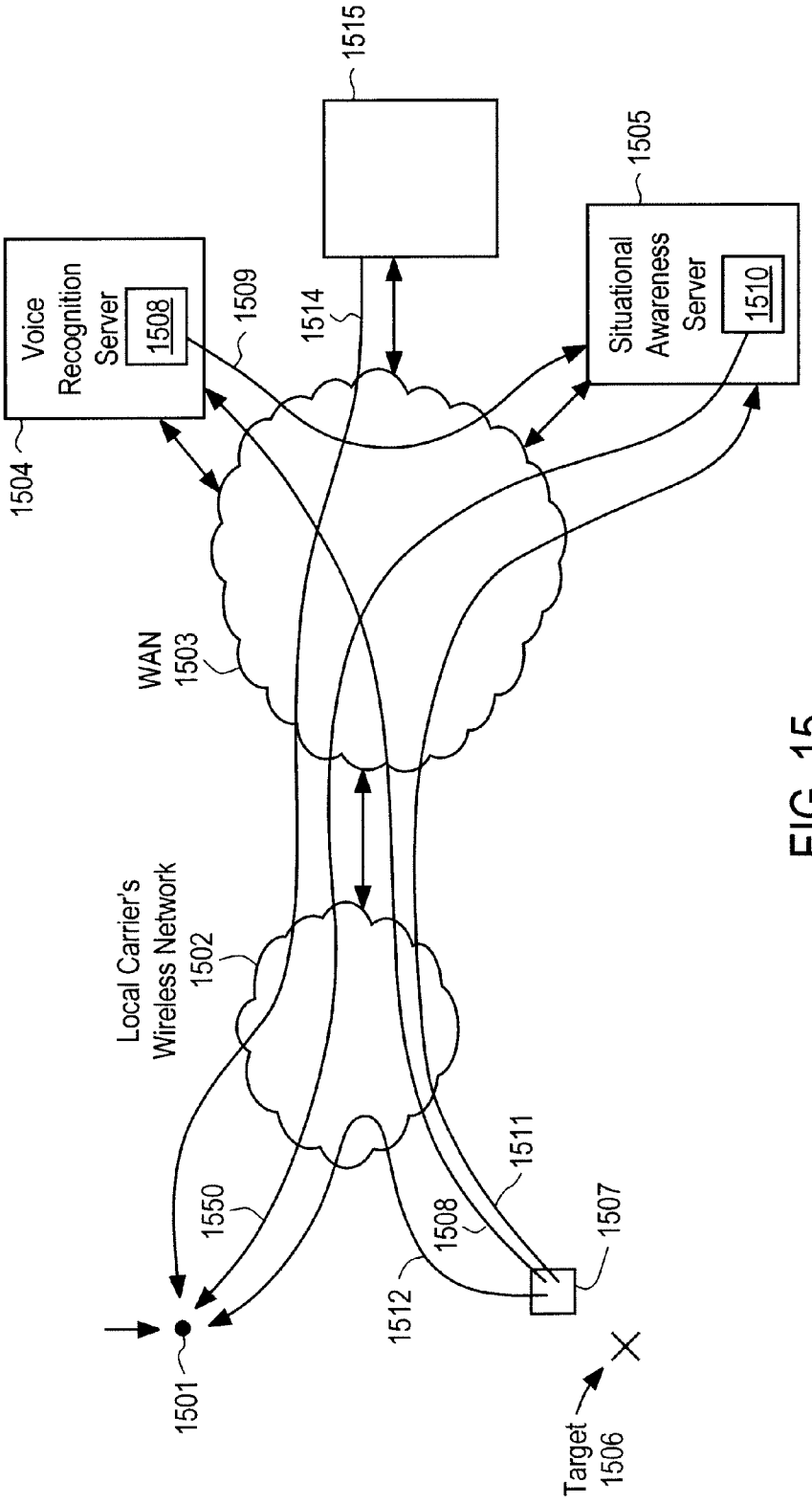
1515
1505
Voice Recognition Server
1508
1509
1514
Situational Awareness Server
1510
1504
WAN
1503
Local Carrier's Wireless Network
1502
1511
1550
1508
1507
1512
1501
Target
1506

FIG. 15

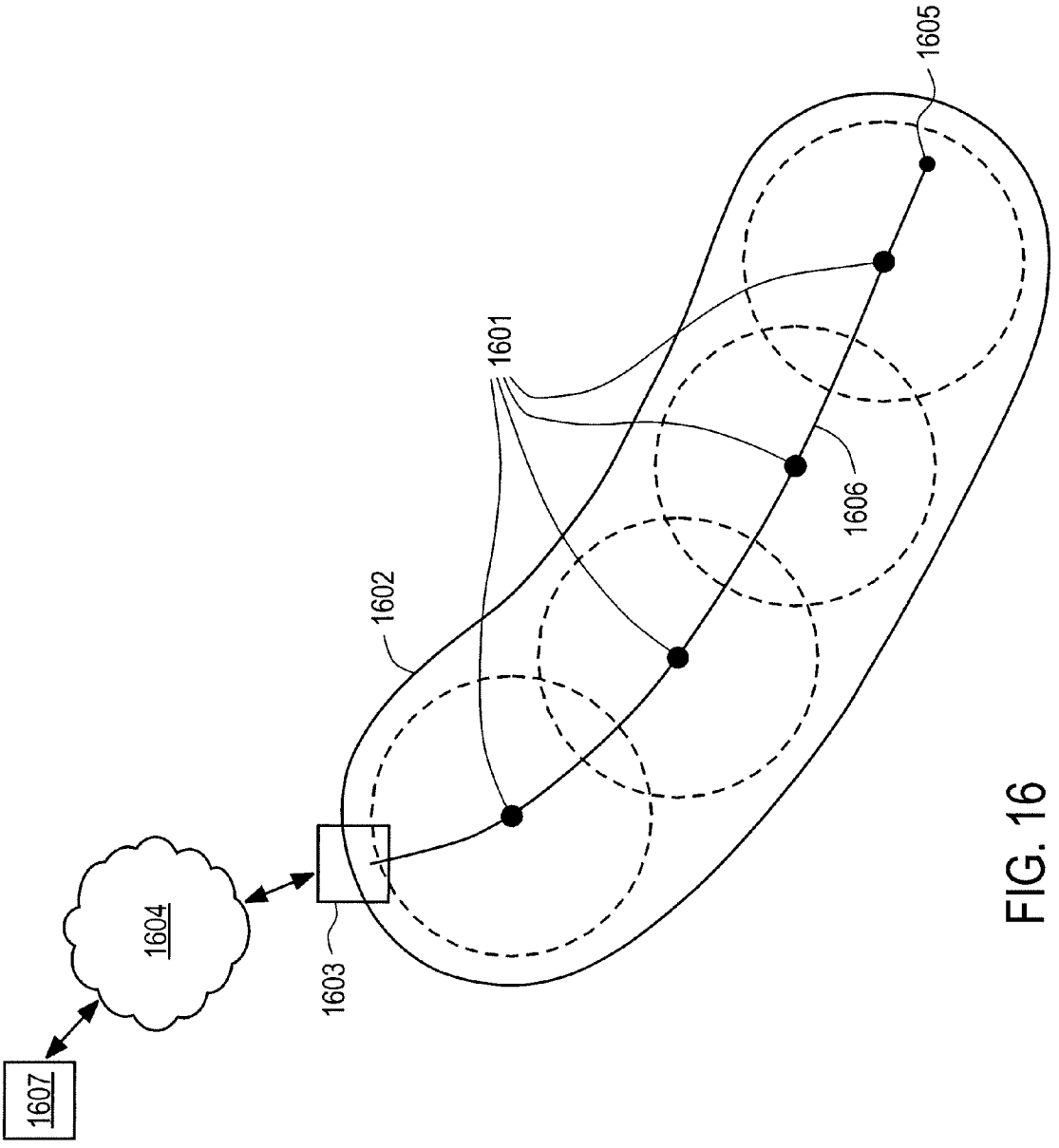

FIG. 16

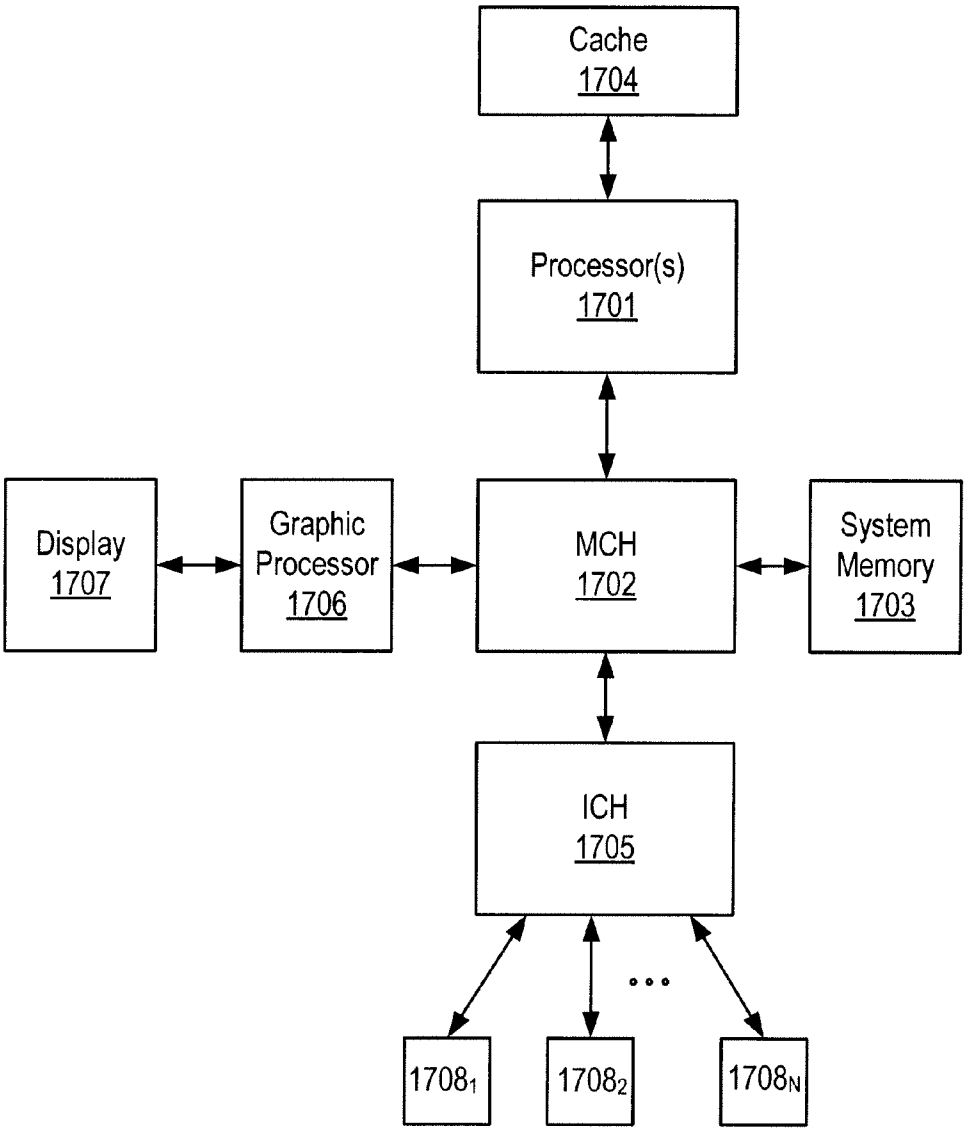
Cache
1704
Processor(s)
1701
Display
1707
Graphic
Processor
1706
MCH
1702
System
Memory
1703
ICH
1705
1708$_1$
1708$_2$
1708$_N$

FIG. 17

INSTANTANEOUS WIRELESS NETWORK ESTABLISHED BY SIMULTANEOUSLY DESCENDING PARAFOILS

CLAIM TO PRIORITY

[0001] The application claims the benefit of U.S. Provisional Application No. 61/324,222 entitled, "Method and System For Optimized Terminal Guidance Of Autonomous Aerial Delivery Systems", filed on Apr. 14, 2010 and U.S. Provisional Application No. 61/324,551 entitled, "Method and System for Improving Touchdown Accuracy Of Aerial Payload Delivery Using Ground Weather Station Uplink", filed on Apr. 15, 2010, and U.S. Provisional Application No. 61/323,792 entitled, "Method and System For Control Of Autonomous Aerial System via GSM Cellular Network", filed on Apr. 13, 2010 and U.S. Provisional Application No. 61/323,750 entitled, "Method and System For Establishing A Short-term Network Mesh Using Miniature Autonomously Guided Parafoils", filed on Apr. 13, 2010 and U.S. Provisional Application No. 61/323,675 entitled, "Method and System For Vertical Replenishment Of Naval Vessels Via Precision Guided Airdrop", filed on Apr. 13, 2010 all of which are also hereby incorporated by reference.

FIELD OF INVENTION

[0002] The field of invention pertains to guided aerial vehicles and more specifically to instantaneous wireless network established by simultaneously descending parafoils.

BACKGROUND

[0003] FIG. **1***a* shows a parafoil **101**. A parafoil is a wing shaped parachute capable of steerable, controlled descent. Essentially, the parachute aspect of the parafoil causes the parafoil to exhibit a gradual descent, while, the wing aspect of the parafoil permits the parafoil to have a guided flight path. The flight path of a parafoil can be controlled by tugging/releasing lines coupled to the left and right trailing edges of the parafoil. Specifically, as observed in FIG. **1***b*, a parafoil can be made to turn to the left if the left trailing edge line **102** is tugged/pulled. Likewise, referring to FIG. **1***c*, a parafoil can be made to turn to the right if the right trailing edge line **103** is tugged/pulled. A parafoil can even be made to momentarily rise, or at least change its pitch upward if both the left and right trailing edge lines **102**, **103** are tugged/pulled.

[0004] Parafoils have been used for guided drops as a consequence of the ability to control their flight path. In order to successfully land a parafoil at or near some target, however, an individual or person is needed to control the trailing edge lines **102**, **103** so as to guide the parafoil with the requisite accuracy. Said another way, the intelligence and sensory abilities of the human brain are needed to manipulate the trailing edge lines **102**, **103** of the parafoil in view of the location of the target, the height of the parafoil, the forward and transverse speeds of the parafoil, the roll, yaw and pitch of the parafoil and the presence of winds.

[0005] Various applications can be envisioned, however, for automatically guided parafoil drops. For instance, consider a situation where a team of catastrophe surveyors/workers/soldiers are in a remote area and in need of certain supplies. Having the ability to simply attach the needed supplies to the parafoil with some computerized intelligence to control the parafoil's trailing edge lines so as to automatically guide the parafoil and its payload in the vicinity of the surveyors/worker/soldiers would obviate the need for keeping skilled parachutists at the ready in case such a need for supplies arises. Moreover, even if skilled parachutists are available and at the ready, a parachutist would be delivered along with the payload. Without the same skills as the surveyors/workers/soldiers, the parachutist is apt to become a burden for the surveyors/workers/soldiers after the payload has been successfully delivered.

BRIEF DESCRIPTION OF THE DRAWINGS

[0006] A better understanding of the present invention can be obtained from the following detailed description in conjunction with the following drawings, in which:

[0007] FIGS. **1***a,b,c* depict a parafoil;

[0008] FIG. **2** shows an embodiment of a parafoil **201** and payload assembly **204**;

[0009] FIG. **3** shows an embodiment of the sensors, motors and control unit within a payload assembly;

[0010] FIG. **4** shows a control system **400** implemented by the control unit's computer system;

[0011] FIG. **5** shows an embodiment of a trajectory plan;

[0012] FIG. **6** shows an embodiment of a methodology executed by a trajectory planning unit during a loitering phase;

[0013] FIG. **7** diagrams an approach for measuring forward speed and wind magnitude;

[0014] FIG. **8** shows an embodiment of a methodology executed by a trajectory planning unit during a downwind phase;

[0015] FIGS. **9***a*,**9***b*,**9***c* pertain to an embodiment of a methodology executed by a trajectory planning unit during a turn phase;

[0016] FIG. **10** pertains to a second embodiment of a methodology executed by a trajectory planning unit during a turn phase;

[0017] FIG. **11** shows a linear wind model and a logarithmic and linear wind model;

[0018] FIG. **12** shows an embodiment of a methodology executed by a trajectory planning unit to calculated a wind model;

[0019] FIGS. **13***a* and **13***b* pertain to an attempt to land a parafoil on a moving target;

[0020] FIGS. **14***a* and **14***b* pertain to a trajectory planning unit that utilizes the model of a vehicle;

[0021] FIG. **15** shows an embodiment of a networked IS that involves a descending parafoil;

[0022] FIG. **16** shows a wireless network established by parafoils;

[0023] FIG. **17** shows a computing system.

DETAILED DESCRIPTION

1.0 Parafoil, Payload Assembly and Control Unit

[0024] FIG. **2** shows an embodiment of a parafoil **201** and payload assembly **204** sufficiently capable of self guidance in a number of situations. The payload assembly **204** includes: i) the payload to be delivered **205** (e.g., supplies to be delivered to workers/soldiers on the ground); ii) sensors **206** to detect, for example, the parafoil's speed and orientation; iii) motors (e.g., actuators) **207***a,b* to "rein in" and "rein out" the left and right trailing lines **202**, **203** in accordance with the parafoil's currently desired direction and orientation; and, iv) a control unit **208** having electronic circuitry to apply the appropriate

control signals to the electronic motors **207***a,b* in response to signals received by the control unit **208** from the sensors **206**. Here, payload assembly **204** may be any mechanical package that physically integrates the payload **205**, sensors **206**, motors **207***a,b* and control unit **208** as a cohesive whole.

[0025] FIG. **3** shows an embodiment of the sensors **306**, motors **307** and control unit **308**. In the embodiment of FIG. **3***a*, the sensors **306** include an internal navigation system (INS) sensor set **312** including: i) three accelerometers **309***a,b,c* to measure linear acceleration in three different, respective directions (x, y, z); ii) three rate gyroscopes **310***a,b,c* to measure angular velocity ($d\theta/dt$, $d\phi/dt$, $d\psi/dt$) along three different axis; and, iii) three magnetometers **311***a,b,c* to sense a three dimensional vector v that defines the parafoil's present pointing. The sensors **306** also include the Global Positioning System (GPS) receiver **312** (to measure the parafoil's location) and barometric altimeter **313** to measure the parafoil's altitude. As is known in the art, an accelerometer output can be integrated once over time to produce a measurement of velocity traveled in the same direction that the acceleration was measured. Likewise, the velocity can be integrated over the same time to determine the distance traveled in the same direction. Similarly, angular velocity as provided by the rate gyroscopes can be integrated over time to determine the number of degrees that have been rotated about the respective axis over the same time period.

[0026] The motors **307**, in an embodiment, include a set of actuators **314***a,b* for the left and right trailing edge lines **302**, **303**. A third actuator **315** is used to release a canopy of the payload assembly after it is dropped from an aircraft so that the parafoil can deploy. The embodiment of FIG. **3** also depicts the control unit **308** as including wireless communication circuitry **316**. Specifically, the control unit **308** includes circuitry **317** to communicate with a local carrier's network (such as GSM circuitry **317** to communicate with a local carrier's GSM network). The wireless communication circuitry **316** may also include wireless circuitry **320** to communicate with a proprietary wireless network or link (e.g., established by the operators of the parafoil).

[0027] As observed, the control unit **306** represents a computer system having a processing core **318** (e.g., microprocessor) and with the sensors **306**, motors **307** and wireless communication circuitry **316** acting as some form of the computing system's I/O. As shown, the sensors **306**, motors **307** and wireless communication circuitry **316** have their own dedicated interfaces (e.g., busses) to the processing core **318** but conceivably communications between the processing core **318** and the different units **306**, **307**, **316** may be shared over a same interface in various combinations. The processing core **318** is coupled to a volatile memory **319** (e.g., DRAM or SRAM) and flash memory **321**. The software executed by the processing core **318** is stored in flash memory **321** and loaded into volatile memory **319** when the control unit is first powered on (in an embodiment, well before the unit is dropped from an airplane). Thereafter the processing core **318** executes the software from volatile memory **319**.

2.0 Control System

[0028] FIG. **4** shows a control system **400** implemented by the control unit's computer system to automatically guide the parafoil's flight. The control system of FIG. **4** includes a trajectory planning unit **401**, a difference unit **402**, a path following unit **404**, the sensors **406** and the motors **407**. The trajectory planning unit **401** is responsible for determining the overall flight path of the parafoil. The flight path essentially defines the parafoil's desired location and orientation at a moment of time. The sensors **406** measure the parafoil's actual location and orientation at the moment of time. The difference unit **402** determines an error signal **403** defined as the difference between the desired and actual location/orientation of the parafoil.

[0029] When there is no difference between the desired and actual location of the parafoil, the parafoil is "on track" and therefore no error signal exists. In this case, the parafoil's traling edge lines do not need to be adjusted. By contrast, when a difference exists between the desired and actual location/orientation of the parafoil, the difference unit **402** produces a substantive error signal **403** that the path following unit **404** reproduces into one or more control signals **405** that are presented to either or both of the motors **407** to adjust the trailing edge lines in a manner that brings the parafoil closer to the desired location/orientation. In various embodiments the trajectory planning unit **401**, difference unit **402** and path following unit **404** are implemented with software program code that is executed by the parafoil's processing core. Other implementations may impose various functions performed by these units in hardware either entirely or partially.

[0030] In an embodiment a model predictive control (MPC) approach is utilized based on a Single-Input Single Output (SISO) discrete system of the form:

$$s_{k+1}=As_k+Bu_k \quad \text{Eqn. 1a}$$

$$p_k=Cs_k \quad \text{Eqn. 1b}$$

where: 1) k is the present state of the parafoil and payload assembly (hereinafter, "parafoil"); 2) k+1 is the next state of the parafoil; 3) A, B and C are matrices that describe the parafoil dynamics; 4) s_k is a vector that describes the present state of the parafoil mechanical system in terms of its roll, change in roll with respect to time, yaw and change in yaw with respect to time; 5) u_k describes the control signals being applied to the parafoil's motors in the present state; and, 6) y_k is the parafoil's trajectory in the present state (that is, the path along which the parafoil is currently headed).

[0031] As provided in Appendix A of the instant application, the above system can be solved for u_k as a function of the parafoil's currently desired trajectory w_k. Thus, for a present parafoil state k, appropriate control u_k to be applied to the parafoil's trailing line motors can be determined to keep the parafoil's path along its desired path w_k.

[0032] Generally, the ability to calculate proper control signals for a desired trajectory is well known in the art. That is, given a desired flight path and an actual deviation from the desired flight path, it is well known (or can be readily determined) how to adjust a parafoil's trailing edge lines to bring the parafoil closer to the flight path. What has heretofore not been known is a generic algorithm or set of algorithms, executable by the parafoil as it is descending, for determining the parafoil's desired flight path to a specific target area where the algorithm takes into account various factors such as the precise location of the target relative to the parafoil when the parafoil is dropped, the altitude at which the parafoil is dropped and the applicable winds. In this respect, the ensuing discussion will focus primarily on algorithms executed by the trajectory planning unit **401**.

[0033] As described in more detail further below, various embodiments exist as to the manner in which the algorithms executed by the trajectory planning unit account for the presence of winds. According to one perspective, the parafoil is

purposely landed into the wind (for the sake of a "soft" landing). As a consequence, the strategy of the parafoil's flight plan is based on establishing a reference inertial trajectory with the major axis being aligned with the direction of prevailing/anticipated/known ground winds. The aloft winds component in this direction dictates the flight plan's logistics, while the crosswind component (measured or unmeasured) is considered as a disturbance. According to one embodiment, the prevailing wind component, estimated at current altitude is assumed to have constant magnitude through the entirety of the parafoil's descent. According to another embodiment the wind is assumed to linearly weaken in terms of magnitude over the course of the parafoil's descent. According to a third embodiment, the wind is assumed to weaken logarithmically over the course of the parafoil's descent. For simplicity, the first embodiment (in which the wind is assumed to have constant magnitude over the course of the parafoil's descent) will be described to provide an overall view of the flight path determination strategy. Subsequently, modifications will be introduced to this basic approach to account for more sophisticated wind modeling.

[0034] As observed in FIG. **4**, the trajectory planning unit **401** receives input information in the form of the target's position **408** (e.g., x, y, z coordinates of the target's position or just x, y if the z position of the target is assumed to be zero) and information concerning the applicable winds **409** and the amount of time (T_{app}) the parafoil is to spend on its "final approach" **410**. As will be discussed further below, the parafoil's flight path as determined by the trajectory planning unit **401** has a plurality of different legs, where, the final approach is the last leg. Here, the final approach time input **410** corresponds to a user input that is set before the parafoil is dropped. In an embodiment where the target is fixed (i.e., is not moving), the target position **408** is also a static input that can be entered before the parafoil is dropped.

[0035] The set of inputs received by the trajectory planning unit **401** also include a dynamic component in the form of a feedback path **411** that exists from the sensors **406** to the trajectory planning unit **401**. In an embodiment, the sensor information that is fed back to the trajectory planning unit **401** at least includes the x, y, z spatial position of the parafoil and its horizontal pointing direction or "yaw" (ψ) (although not all of these parameters are necessarily used at all times during all flight path phases). Here, the flight path determined by the trajectory planning unit **401** need not be static. That is, once a first flight path is determined, the trajectory planning unit **401** is free to change or adjust the flight path as circumstances warrant.

[0036] Referring to FIG. **5**, in an embodiment, the control unit is turned on and operational before the payload assembly with packed parafoil is dropped from an airplane, helicopter or other airborne vehicle at drop point DP. The parafoil is purposely dropped upwind from the target (i.e., so that the wind will initially move the parafoil closer to the target). From the drop point DP, the payload assembly freefalls **500** for a set period of time. During the freefall **500** phase, the flight path control system of FIG. **4** is essentially not activated. Rather, after a first preset time (e.g., 3 seconds) to allow the falling payload assembly to gain some distance from the airborne vehicle it was dropped from, the payload assembly's canopy is opened **501** to release the parafoil. After another preset time period (e.g., 4 seconds) of additional free fall the parafoil is presumed to be fully deployed and its trailing lines untangled **502**.

[0037] At this point, the flight path control system of FIG. **4** becomes operational and in control of the parafoil's flight path for the remainder of the parafoil's descent. As observed in FIG. **5**, the flight path as determined by the trajectory unit **401** includes four major phases **503_1** ("loiter"), **503_2** ("downwind leg"), **503_3** ("turn"), and **503_4** ("final approach"). The flight path is essentially a high level strategy that is believed to be workable across a range of situations and environments. According to one perspective of the strategy, the parafoil is deliberately landed into the wind on the final approach leg **503_4**. That is, when the parafoil is on the final approach **503_4** part of its flight path, the parafoil's flight path direction is opposite that of the wind's direction **520**.

[0038] A rationale for this approach is that when heading into the wind, the responsiveness of the parafoil to control input on its trailing edge lines is enhanced (as compared when the parafoil is heading with the wind) and it provides for a slower landing of the parafoil on the ground so as to protect the payload from the shock of landing. After exiting the initial loitering phase **503_1***b*, the parafoil sails with the wind along the downwind leg **503_2** to a point "D_switch" **506** along the x axis, at which point, the parafoil enters the turn phase **503_3** to turn the parafoil onto its final approach path **503_4**.

2.1 Loitering Phase

[0039] Upon entering the loitering phase **503_1**, the trajectory planning unit maps out a helical descent pattern **504**. In an embodiment the helical descent pattern **504** is defined by points A, B, C and D in x,y space in the proximity of the location where the parafoil is dropped. Each time the parafoil reaches a point sufficiently proximate to one of points A, B, C and D in xy space, the parafoil turns to effect the helical descent. In a further embodiment, points ABCD define a rectangle or square in xy space where two of the rectangle's/square's sides are arranged to be parallel with the wind direction **520**. In various embodiments. The wind direction **520** is entered into the flight control system either before the payload assembly is dropped from the airborne vehicle, or, communicated to the flight control system (e.g., via the control unit's wireless network interface(s)) during its free fall or early loitering state). Points A, B, C, D may also be similarly entered into the flight control system (based on anticipated parafoil dynamics and/or tactical conditions).

[0040] During the helical descent **504** the parafoil accomplishes a number of tasks including: 1) gaining an initial understanding of the parafoil's positioning relative to the target; 2) estimating its correct (weight-specific) performance of the payload system, specifically its forward speed V_h; 3) measuring the wind at its altitude; and, 4) calculating the altitude A_switch **503_1***b* at which the loitering phase **503_1** ends and the downwind leg phase **503_2** begins.

[0041] FIG. **6** shows an embodiment of the algorithm executed by the trajectory planning unit **401** while in the loitering phase in more detail. As observed in FIG. **6**, based on the estimate of V_h the trajectory planning unit calculates the time T_{turn} spent in the turn phase **503_3** and A_switch **507**. Specifically, in an embodiment, first a value of T_{turn} is calculated **601**, then, a value for A_switch is calculated **602**. While these calculations are ensuing, the actual output of the trajectory planning unit **401** corresponds to the ABCD helical descent pattern **504**, so that the trailing edge lines of the parafoil are adjusted as appropriate to keep the parafoil on the ABCD helical descent track.

[0042] As the parafoil descends in the ABCD helical pattern the control unit measures the parafoil's ground speed **603** and, based on these ground speed measurements, estimates the parafoil's air or forward speed (V_h) **604** and the magnitude of the wind (W) at its present altitude **605**. The descent rate (V_v) is also calculated **606**. As observed in FIG. **6**, each of these determinations **604**, **605**, **606** as well as the target location, the preconfigured time of the parafoil's final approach (T_{app}) and the radius (R) of the turn in the turn phase **503_3** can be used to calculate T_{turn} and A_switch **507**. Before discussing these calculations, however, embodiments for making each of the forward speed **604**, wind **605** and descent rate **606** calculations will be discussed first.

[0043] FIG. **7** pertains to the trajectory planning unit's ground speed **603** and wind **604** measurements. In various embodiments, the direction of the prevailing/expected ground wind is entered into or communicated to the parafoil's control unit (e.g., prior to the payload assembly being dropped from the airborne vehicle or through one of the control unit's wireless interfaces after it is dropped). While loitering, the parafoil's control unit determines the prevailing winds along the downwind direction and can also determine the crosswind (much smaller) wind component, which maybe useful during the final turn.

[0044] With the direction of the ground wind (desired landing direction) **520** being known, the trajectory planning unit is able to establish: 1) the direction of the final approach **503**_4; 2) the direction of the downwind leg **503_2** and turn 503_**3**; and, 3) the orientation of the "legs" of the loitering phase's ABCD helical descent. As such, when the loitering phase **503_1** first begins, the trajectory planning unit **401** defines the ABCD helical pattern with straight "out" and "back" legs **701**, **702** that run parallel to the direction **720** of the wind.

[0045] During its descent in the loitering phase, the parafoil will run through one or more straight "out" and "back" legs **701**, **702** of the helical descent. During the run of the parafoil along one of these legs, over time, the trajectory planning unit presents values that correspond to x, y positions along the leg so the parafoil follows the planned leg path. When the parafoil reaches the end of a leg, the trajectory planning unit presents an output that corresponds to a turn so the parafoil can begin to approach its next leg in the pattern. During each pass through a downwind or upwind leg **701**, **702**, the trajectory planning unit measures its ground speed **603** in the direction of the leg. Here, the ground speed of the parafoil in the downwind legs **702** should be faster than the ground speed of the parafoil along the upwind legs **701**.

[0046] The parafoil's air speed (V_h) and the magnitude of the wind (W) can be determined from the opposing measured ground speeds. Specifically,

$(W+V_h)=V1$=ground speed measured in the downwind $(+x)$ direction Eqn. 2a

$W=V1/2-V2/2$=ground speed measured in the upwind $(-x)$ direction Eqn. 2b

such that

$V_h=(V1+V2)/2$ Eqn. 3

$W=V1/2-V2/2$ Eqn. 4.

Multiple wind measurements can be taken through multiple loops of the helical descent (e.g., and averaging them) or only a single wind measurement can be taken through a single loop. Similarly, the crosswind component of the current winds can be estimated while the parafoil travels along two other legs (leg CD and led AB in FIG. **7**). This may be important if the landing is scheduled differently than into the wind. This latter case may be applicable to landing onto a moving target (platform) or delivering payload from a specified direction, not necessarily aligned with a ground wind.

[0047] Referring back to FIG. **6**, the descent rate **606** (V_v) can also be calculated by measuring the parafoil's change in altitude over a period of time. Here, the barometric altimeter readings of INS and/or GPS readings can be used to determine altitude.

[0048] With the estimate provided by Eqn.3, the time T_{turn} expected to be spent in the turn phase **503_3** can be estimated 601 as

$$T_{turn}=\pi R/V_h \quad \text{Eqn. 5}$$

where R is an estimated radius of the turn which, in an embodiment, is a parameter that is entered by a user into the control unit. In another embodiment, the control unit sets an initial value of $R=\Delta Y/2$ where ΔY is the lateral distance along the y axis **511** between the target and the approximate position of the parafoil while loitering. Here, Eqn. 5 essentially corresponds to the time spent in a 180 degree turn with radius R and air speed V_h with a constant turn rate.

[0049] With numerical values being assigned to each of T_{turn}, V_h, V_v, and T_{app}, the parafoil can determine **602** the altitude A_switch at which it exits the loitering phase **503_1** and enters the downwind phase **503_2** as:

$$A_{switch} = V_v^* \frac{L + V_h^*(T_{turn} + 2T_{app}^{des})}{W - V_h^*} \quad \text{Eqn. 6}$$

where, in Eqn. 6, L is the distance separating the parafoil and the target along the x axis. Said another way, L is the x axis intercept of the parafoil'current position. As drawn in FIG. **5**, L is shown approximately as of the moment the parafoil exits the loitering phase. The distance of L "shortens" however as the parafoil draws nearer the target along the x axis in the downwind phase **503_2**. A theoretical discussion and derivation of Eqn. 6 above is provided in Appendix B.

2.2 Downwind Leg Phase

[0050] In an embodiment, once the trajectory planning unit recognizes that the parafoil has descended to an altitude of z=A_switch, the trajectory planning unit switches phases from the loitering phase **503_1** to the downwind leg phase **503_2**. In so doing, the trajectory planning unit changes the desired path of the parafoil from the helical ABCD descent with a line that runs along the x axis positioned at the y axis location of +2R (notably, in situations where the parafoil is to make a right turn in the turn phase **503_3** rather than a left turn, the line is positioned at the y axis location of −2R). As such, while in the downwind leg phase **503_2**, the parafoil simply tracks to the correct y axis location and then, keeping the y axis location fixed as best as practicable, follows the +x axis while descending.

[0051] During its descent along the x axis (during the downwind leg phase **503_2**), the trajectory planning unit continually updates the current winds calculates the position D_switch at which the parafoil should exit the downwind phase **503_2** and enter the turn phase **503_3**. Here, D_switch

is the distance along the x axis between the parafoil and the target at which the parafoil should begin the turn phase. D_switch can be expressed as

$$D_{switch} = -\frac{\hat{z}\left(\hat{V}_h^{*2} - \hat{W}^2\right) + \hat{V}_h^*\hat{V}_v^* T_{turn}\left(\hat{V}_h^* - \hat{W}\right) + \hat{x}\hat{V}_v^*\left(\hat{V}_h^* + \hat{W}\right)}{2\hat{V}_h^*\hat{V}_v^*} \quad \text{Eqn. 7}$$

Notably, the above expression for D_switch is a function of: 1) z, the parafoil's "current" altitude; and 2) x, the parafoil's "current" position along the x axis.

[0052] Recalling the above definitions of D_switch and L, note that the parafoil should begin the turn phase when, substitution of the x and z parameters describing its current position into Eqn. 7 yields D_switch=L=parafoil's current x axis position. As such, as observed in FIG. **8**, during the parafoil's descent along the downwind leg **503_2**, the trajectory planning unit repeatedly calculates **801**, **802** a value for D_switch as a function of its current position. The trajectory planning unit continues to estimate wind W (assuming constant V_h determined via Eqn.3) during the downwind phase and continuously substitutes updated values for them into Eqn. 7 along with the parafoil's positional information. Based on the known V_h (Eqn.3) and measured ground speed V, the current wind is determined as

$$W = V - V_h \quad \text{Eqn. 8}$$

[0053] When the latest calculated value for D_switch is recognized as being sufficiently the same as its present distance (L) along the x axis from the target, the trajectory planning unit exits the downwind leg phase **503_2** and enters the turn phase **503_3**. Notably, the calculated value of D_switch can be negative indicating that the parafoil is to begin its turn before reaching the target's x axis location on the downwind leg. Appendix B also provides a derivation of Eqn. 7.

2.3 Turn Phase

[0054] As discussed above, the decisions made by the trajectory planning unit are based on various measurements (such as forward speed V_h and wind magnitude W) and assumptions (such as a small magnitude for the crosswind component of the wind). Ideally there is no error in such measurements/assumptions, and, when the parafoil reaches the D_switch position and begins its turning phase, not only is the parafoil precisely where the trajectory planning algorithm "hoped" it would be, but also, the winds do not drastically change thereafter. Realistically, however, either or both of these conditions may not materialize. That is, for instance, when the trajectory planning unit decides to enter the turning phase, the parafoil may be "somewhere" in the xy plane other than its targeted location for the specific turn radius R and turn rate over time T_{turn} that the parafoil's trajectory was planned around. Moreover, the winds are constantly changing, which cannot possibly be accounted for during the turn itself. Finally, sudden updrafts and downdrafts may change the descent rate (relative to the ground) and therefore ruin a major estimate of how long the system has to stay in the air.

[0055] FIG. **9***a* shows an example of the former problem (entering turn phase in other than ideal x,y position). Here, representative actual paths **901-905** of the parafoil in the xy plane are different than the ideal planned path **900**. These deviations from the ideal path **900** can result in unwanted error between the target location **910** and the corresponding actual landings **911-915**. FIG. **9***b* shows an example of the later problem (sudden change in wind magnitude W). In this case, the wind has suddenly increased which effectively blows the parafoil short of its target in representative actual paths **921-925**. In each of the representative actual paths **901-905** and **921-925** of FIGS. **9***a* and **9***b*, the trajectory planning unit maps out a simplistic a 180 degree turn over radius R with constant angular rate over T_{turn}.

[0056] FIG. **9***c* shows an improved approach in which the trajectory planning unit calculates an optimum turn based on its current position **950** in the turn relative to the exit point **951** of the turn phase. Here, a two point boundary-value problem is solved by minimizing the "cost" of an arc **952** that spans from the parafoil's current x,y,ψ position **950** (where ψ is the parafoil's yaw angle=the angle at which the parafoil is headed or pointing along the x,y plane) to the x,y,ψ position **951** where the final approach is supposed to start. The "cost" of an arc is determined by N points **953** spaced along the arc in a certain manner and: i) determining the time spent by the parafoil traveling between the points, summing these times to represent the total time spent traversing the arc, and, taking a difference between this total time and T_{turn}; and, ii) determining the yaw rate (angular change of the pointing of the parafoil in the xy plane) beyond a maximum desired yaw rate from each point needed to steer the parafoil to its next point.

[0057] Here, i) above penalizes deviation of the parafoil's total turn time from T_{turn}; and, ii) above penalizes an excessive yaw rate ("sharp turn") needed to accomplish the turn. By formulating the cost as an optimization problem to minimize the cost, the respective positions for a set of N points along an arc between the parafoil's current position and the point where the final approach is to begin will be determined that correspond to an arc whose travel time is closest to T_{turn} and that does not exhibit excessive yaw rate.

[0058] As such, as observed in FIG. **9***c*, the trajectory planning unit determines the position at which the final approach phase is to begin **951** (e.g., in terms of x,y,ψ), and determines its current position **952** (e.g., again in terms of x,y,ψ). With these input parameters, the trajectory planning unit then solves an optimization problem **954** to determine (e.g., x,y) positions of a set of N points **953** that define an arc **902** between the parafoil's current position **952** and the position **951** at which it is to end the turn phase. In one embodiment, the algorithm only optimizes a few parameters pertaining to the initial and final points of the turn. The optimal trajectory is determined analytically. This accelerates trajectory optimization so as to perform optimization about 100 times faster than in real time. This analytically defined inertial reference trajectory is passed to the control unit assuring that the parafoil actually follows he determined arc in flight.

[0059] Notably, the trajectory planning unit is free to repeatedly calculate a new trajectory (and therefore a new set of N points) throughout the turn phase. For example, as observed in FIG. **10**, upon entering the turn phase, the parafoil's trajectory planning unit calculates a first arc/set of N points **1000** that is used to define a first trajectory for the parafoil in the turn phase. Sometime later, for instance, because it is recognized that the parafoil's actual flight path **1002** has substantially deviated from the initial trajectory **1000**, the trajectory planning unit recalculates a second arc/set of N points **1003** that are used to define a second trajectory for the parafoil in the turn phase. In various alternative embodiment, the parafoil automatically (e.g., periodically)

recalculates its trajectory in the turn phase (e.g., without reference to its deviation from an earlier trajectory), or, only calculates a new trajectory if the parafoil's flight path breaches its intended trajectory beyond some threshold. When calculating a new trajectory in the midst of the turn phase some modification is made to the optimization problem to address the fact that the parafoil is not at the beginning of the turn phase (e.g., by comparing the total time in a proposed arc against $T_{turn}-T_{spent}$, where T_{spent} corresponds to the time spent in the turn phase since the turn phase was initiated).

[0060] While optimizing the final turn trajectory, the parafoil's current x,y,ψ position **950** can be determined from the control unit's sensors (e.g., GPS or INS). The (x,y,ψ) position **951** at which the parafoil is to exit the turn phase and enter final approach is defined as:

$$FA=((V_h-W)T_{app},0,-\pi) \quad \text{Eqn. 9}$$

The final turn maneuver is a pertinent part of the guidance algorithm. The parafoil may exit loitering earlier and it can be corrected by delaying the start of the final turn. However, once the final turn maneuver has started, varying the turn rate is the only way to make final corrections to intersect the top of the final approach slope. Varying the turn rate causes the parafoil to do either a steep or shallow turn, but precisely at the top of the final approach, i.e. at the point defined by Eqn.9 in exactly T_{turn} after entering the turn. Only at this final phase can three-dimensional wind disturbances be accounted for by constant reoptimization of the maneuver, i.e. by adjusting T_{turn} and producing a new yaw rate profile.

[0061] Mathematically, the optimization problem can be expressed as

$$J=\left(\sum_{j=1}^{N-1}\Delta t_j - T_{turn}\right)^2+k^{\psi}\Delta \quad \text{Eqn. 10a}$$

$$\Delta=\max_j(0;|\dot{\psi}_j|-\dot{\psi}_{max})^2 \quad \text{Eqn. 10b}$$

where: 1) Δt_j is the time spent by the parafoil traveling from the jth point to the jth+1 point among the arc's N points; 2) k^{ψ} is a scaling factor; 3) ψ_j, is the change in yaw rate at a jth point among the arc's N points; and, 4) ψ_{max} is a desired maximum change in yaw rate. The analytical representation of a trajectory itself is given by

$$\tau_f P'_{\eta}(\bar{\tau})=a_1^{\eta}+2a_2^{\eta}\bar{\tau}+3a_3^{\eta}\bar{\tau}^2+\pi b_1^{\eta}\cos(\pi\bar{\tau})+2\pi b_2^{\eta}\cos(2\pi\bar{\tau})$$

$$\tau_f P''_{\eta}(\bar{\tau})=2a_2^{\eta}+6a_3^{\eta}\bar{\tau}-\pi^2 b\sin(\pi\bar{\tau})-(2\pi)^2 b_2^{\eta}\sin(2\pi\bar{\tau}) \quad \text{Eqn. 11}$$

where $\bar{\tau}=\tau/\tau_f\epsilon[0;1]$ is a scaled abstract argument, a_i^{η} and b_i^{η} (η=1, 2) are coefficients defined by the boundary conditions up to the second-order derivative at $\tau=0$ and $\tau=\tau_f(\bar{\tau}=1)$, and τ_f is a varied parameter. Derivations for Eqns. 10a, 10b, 11 Δt_j, ψ_j, and ψ_{max} can be found in Appendix C. Appendix D provides additional information on the final arc optimization in the case where the wind profile is not constant including a major crosswind component of the wind.

2.4 Final Approach Phase

[0062] Upon the parafoil deciding that it has reached the end of the turn phase (e.g., by recognizing T_{turn} has lapsed since the beginning of the turn phase), the trajectory planning unit produces an output that causes the parafoil to head in the −x direction and maintain that direction until the parafoil lands.

3.0 Improved Wind Models

[0063] The above discussion assumed computation of D_{switch} (Eqn.7), and the final approach point (Eqn.9) based on a constant wind in the x-direction for the entirety of the parafoil's descent. The basic optimization algorithm presented in Appendix C was also based on this assumption, specifically, in one of two kinematic equations describing the horizontal position of the parafoil

$$dx/dt=V_h\cos(\psi t)+W \quad \text{Eqn. 12}$$

A more general optimization algorithm presented in Appendix D, however, removes these assumptions and deals with an arbitrary wind profile based on wind models discussed immediately below.

[0064] Three possible improvements resulting in better assumptions about the wind's behavior from the current altitude all the way down to the ground can be made. A first improvement is based on the assumption that we have multiple parafoils deployed one after another to the same area. Then, a wind profile can be measured by the first system and transmitted to all following systems. A second improvement can be made if we have a ground station that constantly measures ground winds (in the x-direction) and transmits them to all descending parafoils (or a single parafoil) using an RF link or wireless network as described in Section 5. In this case rather than assuming a constant wind, we can model the wind as varying linearly with altitude as shown in FIG. **11** (improvement **1101**). Finally, a third improvement **1102** can be used if no information about the ground winds is available at all. In this case, rather than using a constant wind speed profile, we will model wind magnitude as varying logarithmically with altitude. In any case a new wind profile will be used: i) during the downwind leg to constantly update D_{switch}, i.e. an altitude to start the final turn maneuver (Eqn.7); ii) determine the final approach point given by Eqn.8; iii) determine the turn time T_{turn} of Eqn.5; and iv) determine the turn rate profile during the final turn to be at the final approach point at the prescribed time.

[0065] In the case of the first improvement a three-dimensional altitude-dependent wind profile can be available

$$W(h)=\{W_x(h),W_y(h),W_z(h)) \quad \text{Eqn. 13}$$

Here h is the altitude above the ground while W_x, W_y and W_z are the x-, y- and z-components of the wind. Depending on how this profile was measured it may lack some of the components, i.e. W_z component. Generally speaking, to compute D_{switch}, final approach point and final turn rate profile only x component is needed. Therefore, the only change in Eqns. 7 and 8 will be to substitute the constant wind W with the x-component of so-called ballistic wind W_B, which basically represents the average of winds from a specific altitude all way down to the ground, as explained in Appendix E.

[0066] the case of the second (linear) wind model improvement **1101**, upon exiting the loitering phase the wind profile below the current altitude will be estimated as

$$W(h)=W_0+(m_W)h \quad \text{Eqn. 14}$$

where W_0 is the ground wind as measured at/near the ground (h=0) in the vicinity of the target and m_W is the rate at which the wind magnitude varies with altitude. In an embodiment,

as observed in FIG. **12**, the ground wind term W_0 is provided **1205** to the parafoil (e.g., by being manually or electronically communicated to the parafoil before it is dropped, or, in mid flight after it is dropped such as during the loitering phase). The parafoil's control unit also measures (updates) the wind magnitude **1206** at any altitude W_{h_high} as described above. In order to determine the current altitude, the parafoil's control unit receives a barometric pressure reading from the target **1201** and receives a reading from its own on board barometric altimeter **1202**. With these readings and an altitude reading from the on board GPS system **1203**, the control unit estimates its altitude **1204**. During the downwind leg (if the ground station is available) the value of W_0 may be constantly updated as well as an estimate of W_{h_high}. The parafoil's control unit then calculates **1207** $m_W=(W_{h_high}-W_0)/(h_high)$ where h_high is the altitude at which the wind was measured to be W_{h_high}. Once again, the ballistic wind value W_B (Appendix E) will be used in lieu of W in Eqns. 8 and 9. Other than these modifications, the flight path of the parafoil may be controlled as described in Section 2.0.

[0067] In the case of the third (logarithmic) wind model improvement **1102**, starting from the downwind leg the wind is modeled as

$$W(h)=(m_W)\ln(h/h_0), \text{ when } h\geq h_0 \; (W(h)=0, \text{ when } 0<h<h_0) \quad \text{Eqn. 15}$$

Here, m_W is a coefficient that is defined by the onboard control unit based on the current wind measurements taken at several consequent altitudes using standard regression analysis. Parameter h_0, a small number below 1 meter, is called the "aerodynamic roughness length" and defines the type of terrain around the landing zone and is set before flight. This model needs no prior knowledge of the ground winds. The value of m_W is constantly updated during the downwind leg to come up with more accurate estimates of D_{switch} and the final approach point. Again, the ballistic wind value W_B (Appendix E) is used in lieu of W in Eqns. 8 and 9. Other than these modifications, the flight path of the parafoil may be controlled as described in Section 2.0. Derivations of the coefficient m_W in Eqn. 15 along with analytical dependences for Eqn.8 (which may be used even without computing the ballistic wind) is provided in Appendix F.

4.0 Moving Target

[0068] The discussions above have been directed to an environment where the target is assumed to be a fixed location on the ground. Other applications are envisioned where it may be desirable to land the parafoil on a moving target such as a ship at sea. FIGS. **13***a* and **13***b* pertain to an embodiment where the target is moving in the −x direction (against the wind) and the parafoil is dropped upwind of the moving target at point DP. The target can therefore be stated in two ways which are equated. The first way to define the target is by the difference in its position along the x axis from the moment the parafoil leaves the loitering phase to the moment the parafoil lands.

[0069] This value can be expressed as $x_T-V_T((A_switch)/V_V)$ where V_T is the velocity of the target and A_switch)/V_V is the amount of time expended from the moment the loitering phase is ended to the moment the parafoil lands. Another way to define the target is simply from its earlier definition L as the distance from the parafoil to the target along the x axis. Equating the two expressions, which essentially states that the upon the parafoil exiting the loitering phase the parafoil must move a net distance L along the x axis to land on a moving target that will be at position $x_T-V_T((A_switch)/V_V)$ from its location x_T when the loitering phase was exited yields:

$$L = x_T - \frac{V_T}{V_V} A_{switch} \quad \text{Eqn. 16}$$

The above Eqn for L can be substituted into Eqn. 6 above and solved for A_switch as

$$A_{switch} = V_V \frac{X_T + V_h(T_{turn} + 2T_{app}^{des})}{W - V_h + V_T} \quad \text{Eqn. 17}$$

which expresses the altitude that the parafoil can exit its loitering phase at its location along the x axis within the loitering phase. With the new value of A_switch, the operation of the parafoil may be controlled as described above in Section 2.0. Introduction of improved wind models such as those discussed above with respect to Section 3.0 will yield further changes to the A_switch calculation.

[0070] Another enhancement that may be necessary to accurately land a parafoil on a moving target is the specific location of the landing area on the target itself. For example, referring to FIG. **14***a*, if the target is a moving ship **1400** and its reported position is presumed to be some location **1401** in the middle of the ship at sea level, some pre-processing may be necessary to more accurately define the actual landing area on the ship. In the example of FIG. **14***a*, the appropriate landing area for the parafoil is a rear deck **1404** that is above sea level at the ship's stern **1405**. As such, the "true" landing area target **1406** needs to be offset from the position of the ship **1401** as it is reported to the parafoil's guidance system. Moreover, different ships may have different landing areas as a function of the ship's design. For example, a first type of ship may have its appropriate landing on a read deck as observed in FIG. **14***a* whereas other ships may have its appropriate landing area on a forward deck (toward the bow of the ship) or on a deck in the middle of the ship but more toward the port or starboard sides.

[0071] A possible benefit of the guidance algorithm described in Section 2.0 is that it establishes the reference trajectory in the inertial reference frame. In the case of the moving target (ship, submarine, etc.) this trajectory is tied to the moving target. Therefore, while planning the trajectory it is possible to construct the trajectory so that the parafoil avoids, e.g., a superstructure on the ship's deck. No other known guidance algorithm has this feature.

[0072] In an embodiment, as shown in FIG. **14***b*, the parafoil's control unit includes a data store that models the different kinds of ships that the parafoil may be asked to land on, where, each ship's model effects the necessary modification to the actual target based on the type of ship and also affects the calculations accordingly. In operation, a ship's position, velocity and type are entered or communicated to the parafoil (e.g., before or after it is dropped). The parafoil's trajectory planning unit not only uses the ship's position and velocity to calculate the target but also modifies the equations appropriately in view of the ships' type to more accurately define the target in a manner that is customized to the particular ship.

[0073] In the case of FIG. **14***a*, for example, the fact that the rear deck is raised means that the parafoil will have to exit the loitering phase sooner to keep the guidance calculations consistent. As such, Eqn. 17 would be modified by the trajectory planning unit to be A_switch=[. . .]+z_{ship_x} where z_{ship_x} corresponds to the vertical offset between the precise location where the ship's recognized position x_T at loiter exit is and the height of the rear deck relative to that position. Similarly, Eqn. 16 would be modified by the trajectory planning unit as $L=(x_T-x_{ship})-V_T((A_switch)/V_V)$ to adjust for the fact that the rear deck is behind the ship's recognized position. Lateral changes along the y axis could either affect the loitering position of the parafoil or the radius of the turn R.

[0074] The guidance algorithm features the optimized final turn which allows adjusting the actual landing time. In this case the heave motion of the ship can also be taken into account. This motion can be estimated by the parafoil's control unit based on the altitude above the sea data at the intended touchdown point. Such data can be uplinked to the parafoil using the ground weather station or a GPS unit using network connectivity as described in Section 5.

5.0 Applications of Wireless Network Connectivity to Parafoil Control Unit

[0075] Recall from the discussion of FIG. **3***a* that the control unit may include various wireless interface circuitry, such as first wireless network interface circuitry **317** that is capable of communicating (including transmission and/or reception) over a local carrier's network and/or second wireless network interface circuitry **320** that is capable of communicating over a proprietary network. In various embodiments, the wireless interface circuitry **317**, **320** is used to communicate pertinent information to the parafoil's control unit after the parafoil has been dropped from the airborne vehicle. Examples include, for instance, uploading the ground wind magnitude or the entire winds profile versus altitude along with the ground barometric pressure (to build a wind model as described in Section 3.0), uploading constantly changing target position (such as in the case of a moving ship), including its vertical elevation (to account for a ship's heave motion as described in Section 4.0), a change in a new stationary target location or the new desired landing direction, not necessarily aligned with the ground winds.

[0076] FIG. **15** shows an exemplary information systems (IS) infrastructure for transferring such information to the parafoil. As observed in FIG. **15** an airborne parafoil **1501** is within range of a local carrier's wireless network **1502** such as a tactical cellular GSM network. The local carrier's wireless network **1502** includes a gateway to a wide area network (WAN) **1503** such as the Internet. A voice recognition server **1504** and a situational awareness (SA) server **1505** are each coupled to the WAN **1503** (notably the recognition server **1504** and situational awareness server **1505** may be integrated into a single endpoint).

[0077] According to one embodiment, a command to be given to the airborne parafoil **1501** is verbally spoken, for instance, by an individual on the ground in the vicinity of the parafoil's target **1506** into a handheld and/or portable device **1507** such as a cell phone or smartphone. The verbal command may be any of (but not necessarily limited to) a command to change the target and/or a command to update the ground wind information (e.g., a command to enter a ground wind profile, a command to enter a change in ground wind magnitude and/or ground wind direction, or, a command to change the target to a new location). The verbal command is communicated via a network connection **1508** between the device **1507** and the voice recognition server **1504**.

[0078] The voice recognition server **1504** (e.g., by way of voice recognition software and/or hardware) processes the verbal command and converts the verbal command information into a digital format that is understandable to a computing system. For example if the verbal command was to update the ground wind speed and/or direction, the voice recognition server might create an XML based message or other body of information **1508** in some kind of syntax that is understandable to a computing system. The information **1508** is then sent by way of a network connection **1509** from the voice recognition server **1504** to the situational awareness server **1505**. The situational awareness server **1505** then translates the digitally formatted command **1508** into a packet **1510** that is sent **1550** to the airborne parafoil **1501** over the local carrier's wireless network **1502**.

[0079] In an alternate embodiment, rather than a verbal command being spoken into the device **1507**, the command is instead entered by way of a keyboard or other user interface of the portable device **1507** and sent **1511** by way of a packet to the situational awareness server **1505** or the parafoil directly **1512**. In the former case **1511** where the packet is sent to the situation awareness server first, the situational server sends a packet **1510** having the entered command to the airborne parafoil. In an embodiment, the portable device **1507** may be specialized equipment. For example, the portable device **1507** may be a portable weather station or wind measurement equipment (such as the kind made by Kestrel, Inc. of Sylvan Lake, Mich.) having its own wireless network interface (and/or integrated cell phone and/or smartphone circuitry). In this case, with the same portable device **1507**, wind information can be measured, packetized and sent **1511** to either the situational awareness server **1505** (for subsequent delivery to the airborne parafoil **1501**) or to the airborne parfoil directly **1512**.

[0080] In even further alternate embodiments, a verbal or entered command is made from a command center or other computing system **1551** that is remote from the parafoil's drop zone. For instance, a command **1514** to change the parafoil's target may be made, while the parafoil is in flight, from a computing system **1515** that is coupled to the WAN **1503** many miles away from the parafoil's drop zone. The WAN may be commercial, proprietary, public or some combination thereof and may even have global reach capability. The command may be sent to the parafoil directly **1514**, or, to a situational awareness server beforehand.

[0081] The parafoil may further be configured to transmit into the wireless network **1502** any/all of its measurement information, such as the wind's magnitude at higher altitudes, its ground speed measurements and/or its positional measurements for analysis and/or observation at some endpoint. For instance, according to one embodiment, a plurality of parafoil's are dropped simultaneously over a common area, and, as the parafoils descend (e.g., in a loitering phase), they transmit their locations (and/or ABCD loitering parameters) to a remote command center **1515** that tracks all of the parafoils in flight in real time. An individual or application software then decides, while the parafoils are descending, what their respective targets are. Respective packets are then sent to each of the airborne parafoils informing them of their specific target.

[0082] In another application of a parafoil's ability to transmit measured information into a wireless network, according to one approach a first parafoil is dropped prior to one or more subsequent parafoils. The purpose of the first parafoil is to make wind measurements during its descent and send the measurement results (and/or a wind profile) "up" to the second set of one or more subsequently dropped parafoils. Here, the parafoil can transmit the wind information in the form of one or more packets into the local carrier's network **1502** which redirects (or multicasts or broadcasts) the packet(s) back to each subsequent parafoil. Alternatively, a private wireless link or network can be established between the descending parafoils and the wind information transmitted up to them through the proprietary wireless link.

[0083] To further that point although much of the previous examples discussed the transmission of wireless information to/from an airborne parafoil through a local carrier's wireless network, the same core schemes may be implemented with a proprietary wireless network or link. For example, the portable device **1507** in the vicinity of the target may transmit ground wind information up to a descending parafoil through a proprietary wireless link that is established between the device **1507** and the descending parafoil. Likewise, any packets that are sent to an airborne parafoil may traverse only a proprietary network without any public traffic (up to an including the wireless network) or some combination of proprietary and public traffic networks may be utilized.

[0084] For any of the embodiments discussed above, note that a parafoil may wirelessly transmit its location, altitude and/or high altitude wind information into the network and ultimately to a computing system which executes the trajectory planning unit algorithms (e.g., with other accumulated information such as ground winds, velocity of moving target, etc.). The computing system then sends an updated trajectory plan through the network and wirelessly to the descending parafoil which implements the newly received trajectory plan.

[0085] FIG. **16** shows another approach in which a group of parafoils **1601** are simultaneously descending to establish a temporary wireless network **1602**, for example, between the access point **1603** of an established network **1604** and another remote location **1605** which has no connection to the established network **1604**. For example, if a group of workers or soldiers are at a remote location **1605** (e.g., separated by a mountain range) and a need arises to communicate to them over the established network **1604**, the parafoils **1601** are dropped so as to descend (e.g., in a permanent loitering phase) along an imaginary line **1606** that connects the access point **1603** to the remote location **1605**.

[0086] Apart from wireless network interface circuitry, each of the parafoils **1601** further includes wireless network routing and/or switching software/hardware to route packets. As such, an airborne wireless network is created with each of the parafoils acting as a node of the network. A packet sent from the access point **1603** to the remote location **1605** is relayed by way of nodal hops from parafoil to parafoil until it reaches the remote location **1605**. Likewise, a packet sent from the remote location **1605** is relayed by way of nodal hops from parafoil to parafoil in the reverse direction until it reaches the access point **1603**. The parafoils **1601** may include nearest neighbor or other awareness technology that permit them to periodically update configure (e.g., by way of periodic updates) their routing tables mid flight (e.g., forming a so-called mesh network), or, the nodal configuration and routing tables may be predetermined ahead of time. The drop pattern and/or guidance systems may be used to orient each of the parafoils in its proper nodal position.

[0087] Whether the individuals at the remote location **1605** are aware of the establishment of the temporary network in their direction may depend on the circumstances. For instance, if a verbal communication needs to take place between individuals at some command center **1607** coupled to the established network **1604** and the individuals at the remote location **1605**, the parafoils **1601** may be equipped with transmission circuitry that transmits a signal to equipment held by the personnel at the remote location **1605** that triggers some kind of alarm that an imminent verbal communication is being arranged. By contrast, if only an electronic message is to be delivered to the remote personnel, such as an email, no alarm need be triggered ahead of time.

[0088] The above discussion spoke of the network established by the parafoils as being temporary in the sense that the network is torn down or otherwise made unworkable prior to or approximately at the time of the landing of the parafoils. A temporary network is useful where, for instance, the safety or security of the remote team **1605** is comprised by the presence of the network. For example, continued transmissions by the parafoil/nodes might lead to the unwanted discovery of the network and the remote individuals. Other circumstances may arise where a permanent network is desired. In this case, the parafoil/nodes can continue to operate to implement a wireless network long after the parafoils have landed.

[0089] Lastly, that FIG. **16** is simplistic in that only a single line **1606** is drawn to connect to a single access node **1603** to a single emote location **1605**. In actuality the "line" may take any shape suitable to connect an access point to a remote location (e.g., curved, triangular, etc.). Moreover, the parafoil implemented network may reach more than one access point and/or more than one remote location by arranging multiple lines/branches as appropriate. Conceivably, a cental core of parafoils may form a short-term network backbone and branches of parafoils extended along lines stemming from the backbone/core may reach out to various established network access points and/or remote locations.

[0090] FIG. **17** shows an embodiment of a computing system (e.g., a computer). The exemplary computing system of FIG. **17** includes: 1) one or more processing cores **1701** that may be designed to include two and three register scalar integer and vector instruction execution; 2) a memory control hub (MCH) **1702**; 3) a system memory **1703** (of which different types exist such as DDR RAM, EDO RAM, etc,); 4) a cache **1704**; 5) an I/O control hub (ICH) **1705**; 6) a graphics processor **1706**; 7) a display/screen **1707** (of which different types exist such as Cathode Ray Tube (CRT), flat panel, Thin Film Transistor (TFT), Liquid Crystal Display (LCD), DPL, etc.) one or more I/O devices **1708**.

[0091] The one or more processing cores **1701** execute instructions in order to perform whatever software routines the computing system implements. The instructions frequently involve some sort of operation performed upon data. Both data and instructions are stored in system memory **1703** and cache **1704**. Cache **1704** is typically designed to have shorter latency times than system memory **1703**. For example, cache **1704** might be integrated onto the same silicon chip(s) as the processor(s) and/or constructed with faster SRAM cells whilst system memory **1703** might be constructed with slower DRAM cells. By tending to store more frequently used instructions and data in the cache **1704** as

opposed to the system memory **1703**, the overall performance efficiency of the computing system improves.

[0092] System memory **1703** is deliberately made available to other components within the computing system. For example, the data received from various interfaces to the computing system (e.g., keyboard and mouse, printer port, LAN port, modem port, etc.) or retrieved from an internal storage element of the computing system (e.g., hard disk drive) are often temporarily queued into system memory **1703** prior to their being operated upon by the one or more processor(s) **1701** in the implementation of a software program. Similarly, data that a software program determines should be sent from the computing system to an outside entity through one of the computing system interfaces, or stored into an internal storage element, is often temporarily queued in system memory **1703** prior to its being transmitted or stored.

[0093] The ICH **1705** is responsible for ensuring that such data is properly passed between the system memory **1703** and its appropriate corresponding computing system interface (and internal storage device if the computing system is so designed). The MCH **1702** is responsible for managing the various contending requests for system memory **1703** access amongst the processor(s) **1701**, interfaces and internal storage elements that may proximately arise in time with respect to one another.

[0094] One or more I/O devices **1708** are also implemented in a typical computing system. I/O devices generally are responsible for transferring data to and/or from the computing system (e.g., a networking adapter); or, for large scale non-volatile storage within the computing system (e.g., hard disk drive or semiconductor non volatile storage device that is the main store for the system's program code when the system is powered off). ICH **1705** has bi-directional point-to-point links between itself and the observed I/O devices **1708**.

[0095] Processes taught by the discussion above may be performed with program code such as machine-executable instructions that cause a machine that executes these instructions to perform certain functions. In this context, a "machine" may be a machine that converts intermediate form (or "abstract") instructions into processor specific instructions (e.g., an abstract execution environment such as a "virtual machine" (e.g., a Java Virtual Machine), an interpreter, a Common Language Runtime, a high-level language virtual machine, etc.)), and/or, electronic circuitry disposed on a semiconductor chip (e.g., "logic circuitry" implemented with transistors) designed to execute instructions such as a general-purpose processor and/or a special-purpose processor. Processes taught by the discussion above may also be performed by (in the alternative to a machine or in combination with a machine) electronic circuitry designed to perform the processes (or a portion thereof) without the execution of program code.

[0096] It is believed that processes taught by the discussion above may also be described in source level program code in various object-orientated or non-object-orientated computer programming languages (e.g., Java, C#, VB, Python, C, C++, J#, APL, Cobol, Fortran, Pascal, Perl, etc.) supported by various software development frameworks (e.g., Microsoft Corporation's .NET, Mono, Java, Oracle Corporation's Fusion, etc.). The source level program code may be converted into an intermediate form of program code (such as Java byte code, Microsoft Intermediate Language, etc.) that is understandable to an abstract execution environment (e.g., a Java Virtual Machine, a Common Language Runtime, a high-level language virtual machine, an interpreter, etc.) or may be compiled directly into object code.

[0097] According to various approaches the abstract execution environment may convert the intermediate form program code into processor specific code by, 1) compiling the intermediate form program code (e.g., at run-time (e.g., a JIT compiler)), 2) interpreting the intermediate form program code, or 3) a combination of compiling the intermediate form program code at run-time and interpreting the intermediate form program code. Abstract execution environments may run on various operating systems (such as UNIX, LINUX, Microsoft operating systems including the Windows family, Apple Computers operating systems including MacOS X, Sun/Solaris, OS/2, Novell, etc.).\

[0098] An article of manufacture may be used to store program code. An article of manufacture that stores program code may be embodied as, but is not limited to, one or more memories (e.g., one or more flash memories, random access memories (static, dynamic or other)), optical disks, CD-ROMs, DVD ROMs, EPROMs, EEPROMs, magnetic or optical cards or other type of machine-readable media suitable for storing electronic instructions. Program code may also be downloaded from a remote computer (e.g., a server) to a requesting computer (e.g., a client) by way of data signals embodied in a propagation medium (e.g., via a communication link (e.g., a network connection)).

[0099] In the foregoing specification, the invention has been described with reference to specific exemplary embodiments thereof. It will, however, be evident that various modifications and changes may be made thereto without departing from the broader spirit and scope of the invention as set forth in the appended claims. The specification and drawings are, accordingly, to be regarded in an illustrative rather than a restrictive sense.

[00100] Appendix A

Model Predictive Control

Consider a simple Single-Input Single-Output (SISO) discrete system described in state space form as:

$$\begin{aligned} \mathbf{x}_{k+1} &= \mathbf{A}\mathbf{x}_k + \mathbf{B}u_k \\ y_k &= \mathbf{C}\mathbf{x}_k \end{aligned} \tag{1}$$

(Hereinafter bold font for lower-case symbols denotes vectors and bold font for upper-case symbols denotes matrices). Assume that the system matrices **A**, **B**, and **C** are known and that $\mathbf{x}_k$ is the state vector, u_k is the control input, and y_k is the output at time k. The model described above can be used to estimate the future state of the system. Assuming a desired trajectory w_k is known an estimated error signal $\hat{e}_k = w_k - \hat{y}_k$ is computed over a finite set of future time instants called the prediction horizon, H_p (hereinafter the symbol "^" is used to represent an estimated quantity). In model predictive control, the control computation problem is cast as a finite time discrete optimal control problem. To compute the control input at a given time instant, a quadratic cost function is minimized through the selection of the control history over the control horizon. The cost function can be written as:

$$J = \left(\mathbf{W} - \hat{\mathbf{Y}}\right)^T \mathbf{Q}\left(\mathbf{W} - \hat{\mathbf{Y}}\right) + \mathbf{U}^T\mathbf{R}\mathbf{U}, \tag{2}$$

where

$$\mathbf{W} = [w_{k+1}, w_{k+2}, \ldots, w_{k+H_p}]^T, \tag{3}$$

$$\hat{\mathbf{Y}} = \mathbf{K}_{CA}\mathbf{x}_k + \mathbf{K}_{CAB}\mathbf{U}, \tag{4}$$

$$\mathbf{U} = [u_k, u_{k+1}, \ldots, u_{k+H_p-1}]^T, \tag{2}$$

and both **R** and **Q** are symmetric positive semi-definite matrices of size H_p x H_p. Equation 1 is used to express the predicted output vector $\hat{\mathbf{Y}}$ in terms of the system matrices

$$\mathbf{K}_{CA} = \begin{bmatrix} \mathbf{CA} \\ \mathbf{CA}^2 \\ \vdots \\ \mathbf{CA}^{H_p} \end{bmatrix}, \tag{6}$$

$$\mathbf{K}_{CAB} = \begin{bmatrix} \mathbf{CB} & 0 & 0 & 0 & 0 \\ \mathbf{CAB} & \mathbf{CB} & 0 & 0 & 0 \\ \mathbf{CA}^2\mathbf{B} & \mathbf{CAB} & \mathbf{CB} & 0 & 0 \\ \vdots & \vdots & \vdots & \ddots & 0 \\ \mathbf{CA}^{H_p-1}\mathbf{B} & \cdots & \mathbf{CA}^2\mathbf{B} & \mathbf{CAB} & \mathbf{CB} \end{bmatrix}. \quad (7)$$

The first term in Eq.(2) penalizes tracking error, while the second term penalizes control action. Equations (2), (6), and (7) can be combined resulting in the cost function

$$J = \left(\mathbf{W} - \mathbf{K}_{CA}\mathbf{x}_k - \mathbf{K}_{CAB}\mathbf{U}\right)^T \mathbf{Q}\left(\mathbf{W} - \mathbf{K}_{CA}\mathbf{x}_k - \mathbf{K}_{CAB}\mathbf{U}\right) + \mathbf{U}^T\mathbf{R}\mathbf{U} \quad (8)$$

that is now expressed in terms of the system state $\mathbf{x}_k$, desired trajectory **W**, control vector **U** and system matrices **A**, **B**, **C**, **Q**, and **R**.

The control **U**, which minimizes Eq.(8), can be found analytically as

$$\mathbf{U} = \mathbf{K}\left(\mathbf{W} - \mathbf{K}_{CA}\mathbf{x}_k\right), \quad (9)$$

where

$$\mathbf{K} = \left(\mathbf{K}_{CAB}^T\mathbf{Q}\mathbf{K}_{CAB} + \mathbf{R}\right)^{-1}\mathbf{K}_{CAB}^T\mathbf{Q}. \quad (10)$$

Equation 10 contains the optimal control inputs over the entire control horizon, however at time *k* only the first element u_k is needed. The first element u_k can be extracted from Eq.(9) by defining $\mathbf{K}_1$ as the first row of **K**. The optimal control over the next time sample becomes

$$u_k = \mathbf{K}_1\left(\mathbf{W} - \mathbf{K}_{CA}\mathbf{x}_k\right), \quad (11)$$

where calculation of the first element of the optimal control sequence requires the desired trajectory **W** over the prediction horizon and the current state $\mathbf{x}_k$.

Parafoil Modeling

The full combined flexible system of the parafoil canopy and the payload can be represented as a 9 or 8 degree-of-freedom (DoF) model depending on the specific harness connecting these two pieces together. Alternatively it can also be modeled as a solid structure requiring only six-DoF, which include three inertial position components of the system mass center as well as the three Euler orientation angles of the parafoil-payload system. This section first introduces a six-DoF model of a generic parafoil system that will be used for simulation and GNC algorithm development, and then addresses a simplified model used to compute the MPC gains appearing in Eq.(11).

A. Six DoF Model

Figure A shows a schematic of a parafoil and payload system. With the exception of movable parafoil brakes, the parafoil canopy is considered to be a fixed shape once it has completely inflated. A body frame {*B*} is fixed at the system mass center with the unit vectors $\mathbf{i}_B$ and $\mathbf{k}_B$ orientated forward and down. Orientation of the parafoil canopy with respect to the body frame is defined as the incidence angle *Γ*.

Orientation of the body frame {*B*} is obtained by a sequence of three body-fixed rotations. Starting from the inertial frame {*I*}, the system is successively rotated through Euler yaw ψ, pitch ϑ, and roll φ. The resulting transformation from the inertial to body frame is

$$\mathbf{T}_{IB} = \begin{bmatrix} c_\theta c_\psi & c_\theta s_\psi & -s_\theta \\ s_\phi s_\theta c_\psi - c_\phi s_\psi & s_\phi s_\theta s_\psi + c_\phi c_\psi & s_\phi c_\theta \\ c_\phi s_\theta c_\psi + s_\phi s_\psi & c_\phi s_\theta s_\psi - s_\phi c_\psi & c_\phi c_\theta \end{bmatrix}, \tag{12}$$

where the common shorthand notation for trigonometric functions is employed, so that for any angle α $\sin(\alpha) \equiv s_\alpha$ and $\cos(\alpha) \equiv c_\alpha$. Translation kinematics of the system become

$$\begin{bmatrix} \dot{x} \\ \dot{y} \\ \dot{z} \end{bmatrix} = \mathbf{T}_{IB}^{T} \begin{bmatrix} u \\ v \\ w \end{bmatrix}, \tag{13}$$

where *x*, *y*, and *z* are the inertial positions and *u*, *v*, and *w* are body frame velocities. Defining the angular velocity of the parafoil payload system as:

$$\boldsymbol{\omega}_{B/I} = p\mathbf{i}_B + q\mathbf{j}_B + r\mathbf{k}_B \tag{14}$$

results in the following rotational kinematics equations:

$$\begin{bmatrix} \dot{\phi} \\ \dot{\theta} \\ \dot{\psi} \end{bmatrix} = \begin{bmatrix} 1 & s_\phi t_\theta & c_\phi t_\theta \\ 0 & c_\phi & -s_\phi \\ 0 & s_\phi c_\theta^{-1} & c_\phi c_\theta^{-1} \end{bmatrix} \begin{bmatrix} p \\ q \\ r \end{bmatrix} \tag{15}$$

($t_\alpha \equiv \tan(\alpha)$).

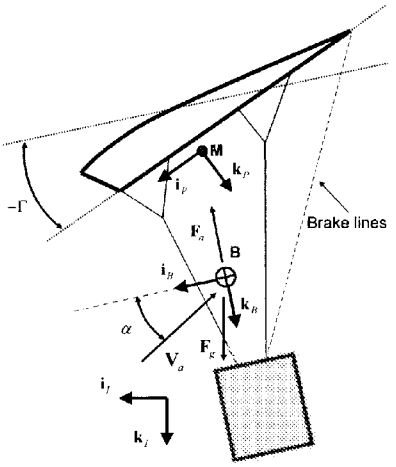

Fig. A A generic 6-DoF parafoil-payload system.

Forces and moments acting on the parafoil and payload have contributions from: weight, aerodynamic loads, and apparent mass of the canopy. Weight contribution of the system is expressed in the body frame,

$$\mathbf{F}_g = \begin{bmatrix} -s_\theta \\ s_\phi c_\theta \\ c_\phi c_\theta \end{bmatrix} mg, \tag{16}$$

with m being the system mass and g the acceleration from gravity. Aerodynamic forces and moments have contributions from both the canopy and payload. Both canopy and payload contributions are combined into a single aerodynamic model using standard aerodynamic derivatives. The aerodynamic force is modeled as:

$$\mathbf{F}_a = \mathbf{T}_{AB}\frac{\rho V_a^2 S_p}{2}\begin{bmatrix} C_{D0}+C_{D\alpha 2}\alpha^2 \\ C_{Y\beta}\beta \\ C_{L0}+C_{L\alpha}\alpha \end{bmatrix}, \tag{17}$$

where; α and β are the angle of attack and sideslip of the body frame, V_a is the true airspeed, S_p is the parafoil canopy area, and $\mathbf{T}_{AB}$ is the transformation from the aerodynamic to body frame by the angle of attack α. Similarly, the aerodynamic moment is written as:

$$\mathbf{M}_a = \frac{\rho V_a^2 S_p}{2}\begin{bmatrix} b(C_{l\beta}+\frac{b}{2V_a}C_{lp})+\frac{b}{2V_a}C_{lr}r+\bar{d}^{-1}C_{l\delta a}\delta_a) \\ \bar{c}(C_{m0}+C_{m\alpha}\alpha+\frac{\bar{c}}{2V_a}C_{mq}q) \\ b(C_{n\beta}+\frac{b}{2V_a}C_{np}p+\frac{b}{2V_a}C_{nr}r+\bar{d}^{-1}C_{n\delta a}\delta_a) \end{bmatrix} \tag{18}$$

where, b and $\bar{c}$ are the canopy span and chord, δ_a is the asymmetric brake deflection, and $\bar{d}$ is the maximum brake deflection. Parafoil canopies with small mass to volume ratios can experience large forces and moments from accelerating fluid called "apparent mass." They appear as additional mass and inertia values in the final equations of motion. Parafoil canopies with small arch-to-span ratios and negligible camber can be approximated to useful accuracy by an ellipsoid having three planes of symmetry; however, the planes of symmetry in the canopy frame may not be aligned with the body frame, as shown in Fig. A. Apparent mass forces and moments for an approximately ellipsoidal canopy can be conveniently defined using the translation and angular velocities expressed in the canopy frame {P}. Defining $\mathbf{T}_{BP}$ as the single axis transformation from the body to canopy reference frame by the incidence angle Γ, $\mathbf{r}_{BM}=[x_{BM}, y_{BM}, z_{BM}]^T$ as the vector from the system mass center to the apparent mass center, and $\mathbf{W}$ as the wind vector, the velocity of the canopy at the apparent mass center can be expressed in the canopy frame as:

$$\begin{bmatrix}\tilde{u}\\ \tilde{v}\\ \tilde{w}\end{bmatrix} = \mathbf{T}_{BP}\left(\begin{bmatrix}u\\ v\\ w\end{bmatrix}+\mathbf{S}_{\boldsymbol{\omega}}^{B}\begin{bmatrix}x_{BM}\\ y_{BM}\\ z_{BM}\end{bmatrix}-\mathbf{T}_{IB}\mathbf{W}\right), \tag{19}$$

where the second term represents the vector cross product using the skew-symmetric matrix $\mathbf{S}_{\omega}^{B}$, constructed as follows:

$$\mathbf{S}_{\boldsymbol{\xi}}^{A}=\begin{bmatrix}0 & -\xi_z & \xi_y\\ \xi_z & 0 & -\xi_x\\ -\xi_y & \xi_x & 0\end{bmatrix} \tag{20}$$

(here ξ_x, ξ_y and ξ_z are the components of vector $\boldsymbol{\xi}$ expressed in a coordinate frame {A}).

Similarly, the angular velocity expressed in the canopy frame {P} becomes

$$\begin{bmatrix}\tilde{p}\\ \tilde{q}\\ \tilde{r}\end{bmatrix} = \mathbf{T}_{BP}\begin{bmatrix}p\\ q\\ r\end{bmatrix}. \tag{21}$$

Forces and moments from apparent mass and inertia are then found by relating the fluid's kinetic energy to resultant forces and moments. Apparent mass and inertia contributions expressed in the body frame can be written as:

$$\mathbf{F}_{a.m.} = -\mathbf{T}_{BP}^{T}\left(\mathbf{I}_{a.m.}\begin{bmatrix}\dot{\tilde{u}}\\ \dot{\tilde{v}}\\ \dot{\tilde{w}}\end{bmatrix}+\mathbf{S}_{\boldsymbol{\omega}}^{P}\mathbf{I}_{a.m.}\begin{bmatrix}\tilde{u}\\ \tilde{v}\\ \tilde{w}\end{bmatrix}\right), \tag{22}$$

$$\mathbf{M}_{a.i.} = -\mathbf{T}_{BP}^{T}\left(\mathbf{I}_{a.i.}\begin{bmatrix}\dot{\tilde{p}}\\ \dot{\tilde{q}}\\ \dot{\tilde{r}}\end{bmatrix}+\mathbf{S}_{\boldsymbol{\omega}}^{P}\mathbf{I}_{a.i.}\begin{bmatrix}\tilde{p}\\ \tilde{q}\\ \tilde{r}\end{bmatrix}\right), \tag{23}$$

where

$$\mathbf{I}_{a.m.}=\begin{bmatrix}A & 0 & 0\\ 0 & B & 0\\ 0 & 0 & C\end{bmatrix} \text{ and } \mathbf{I}_{a.i.}=\begin{bmatrix}P & 0 & 0\\ 0 & Q & 0\\ 0 & 0 & R\end{bmatrix}. \tag{24}$$

Apparent mass and inertia values *A*, *B*, *C*, *P*, *Q*, and *R* appearing in Eq.(24) can be calculated for known simple shapes or can be approximated as discussed in Lissaman, P., and Brown, G., "Apparent Mass Effects on Parafoil Dynamics," AIAA Paper 93-1236, May 1993.

Dynamic equations are formed by summing forces and moments about the system mass center, both in the body reference frame, and equating to the time derivative of linear and angular momentum. Final dynamic equations of motion are expressed compactly in matrix form below, where for the quantities in Eq.(24) the common convention is used for tensors of second rank such that $\mathbf{I}'_{\xi}=\mathbf{T}_{BP}^{T}\mathbf{I}_{\xi}\mathbf{T}_{BP}$:

$$\begin{bmatrix} m\mathbf{I}_{3\times3}+\mathbf{I}'_{a.m.} & \cdots & -\mathbf{I}'_{a.m.}\mathbf{S}^{B}_{\mathbf{r}_{BM}} \\ \cdots & \cdots & \cdots \\ \mathbf{S}^{B}_{\mathbf{r}_{BM}}\mathbf{I}'_{a.m.} & \cdots & \mathbf{I}+\mathbf{I}'_{a.i.}-\mathbf{S}^{B}_{\mathbf{r}_{BM}}\mathbf{I}'_{a.m.}\mathbf{S}^{B}_{\mathbf{r}_{BM}}\end{bmatrix}\begin{bmatrix}\dot{u}\\ \dot{v}\\ \dot{w}\\ \cdots\\ \dot{p}\\ \dot{q}\\ \dot{r}\end{bmatrix}=\begin{bmatrix}\mathbf{F}\\ \cdots\\ \mathbf{M}\end{bmatrix}, \tag{25}$$

where $\mathbf{I}_{3\times3}$ is the identity matrix, $\mathbf{I}=\begin{bmatrix}I_{xx} & 0 & I_{xz}\\ 0 & I_{yy} & 0\\ I_{xz} & 0 & I_{zz}\end{bmatrix}$,

$$\mathbf{F}=\mathbf{F}_{a}+\mathbf{F}_{g}-m\mathbf{S}^{B}_{\boldsymbol{\omega}}\begin{bmatrix}u\\ v\\ w\end{bmatrix}-\mathbf{T}_{BP}^{T}\mathbf{S}^{P}_{\boldsymbol{\omega}}\mathbf{I}_{a.m.}\begin{bmatrix}\tilde{u}\\ \tilde{v}\\ \tilde{w}\end{bmatrix}-\mathbf{I}'_{a.m.}\mathbf{S}^{B}_{\boldsymbol{\omega}}\mathbf{T}_{IB}\mathbf{W}, \tag{26}$$

$$\mathbf{M}=\mathbf{M}_{a}-\mathbf{S}^{B}_{\boldsymbol{\omega}}\mathbf{I}\begin{bmatrix}p\\ q\\ r\end{bmatrix}-\mathbf{S}^{B}_{\mathbf{r}_{BM}}\mathbf{T}_{BP}^{T}\mathbf{S}^{P}_{\boldsymbol{\omega}}\mathbf{I}_{a.m.}\begin{bmatrix}\tilde{u}\\ \tilde{v}\\ \tilde{w}\end{bmatrix}-\mathbf{T}_{BP}^{T}\mathbf{S}^{P}_{\boldsymbol{\omega}}\mathbf{I}_{a.i.}\begin{bmatrix}\tilde{p}\\ \tilde{q}\\ \tilde{r}\end{bmatrix}+\mathbf{S}^{B}_{\mathbf{r}_{BM}}\mathbf{I}'_{a.m.}\mathbf{S}^{B}_{\boldsymbol{\omega}}\mathbf{T}_{IB}\mathbf{W}. \tag{27}$$

[0101] Appendix B

Terminal Guidance

The last three phases introduced in Appendix A (Phases 4-6) are the most critical stages of parafoil guidance. The system must be dropped up wind of the target to ensure it can be reached, however, it is desired to impact the target traveling into the wind to reduce ground speed. In addition it is beneficial to arrive near the target with excess altitude in order to make final guidance decisions. Finally, there is a very strict time limitation. The ADS can be slightly late or earlier departing/arriving to all other phases, but this last Phase 6 ends sharply at landing. All this means that special precautions have to be made in building a control algorithm for the terminal phase.

First, assume that there is no cross wind component, i.e. that the ground winds uploaded to the system before deployment have not changed. An ideal terminal guidance trajectory can be defined as outlined in Fig. B, where the following notations are used (Fig. B represents the left approach pattern, but everything will be the same for the right pattern as well.):

x, y, z – a standard right-handed North-East-Down coordinate frame with the origin at the target;

t_{start} – time corresponding to the beginning of the downwind leg (Phase 4);

t_0 – time corresponding to the beginning of the final 180°-turn (Phase 5);

t_1 – time corresponding to intercepting the final approach (Phase 6);

t_{exit} – time when guidance switches from Phase 5 to Phase 6;

t_2 – time of touchdown;

L – distance away from the target line;

D_{switch} – optimal distance to pass the target (initiating a final turn at t_0 should achieve the desired impact location);

$T_{turn} = t_1 - t_0$ – final turn time;

$T_{app} = t_2 - t_1$ – final approach time, determining t_0 and D_{switch} (a large value allows correction for terminal errors and reduces errors from changing winds, while a small value reduces errors during final approach);

R – final turn radius;

W – wind (positive when coming from the x_I direction and negative as shown in Fig. B);

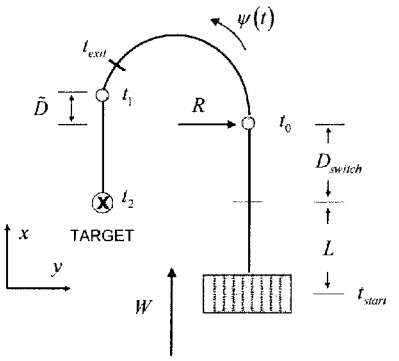

Fig. B Terminal guidance maneuver.

$\psi(t)$ – final turn function for parafoil to track during the final turn;

$\tilde{D} = WT_{turn}$ – distance defined by imperfection (asymmetry) of the final turn because of the wind.

The terminal guidance problem can be summarized as follows. For a parafoil in the presence of wind *W*, at altitude z, and a distance *L* from the target, find the distance D_{switch} to the final turn initiation point (TIP), required to travel past the target for an ideal impact at t_2 (of course, D_{switch} is a function of the desired T_{app}^{des}.)

In general, the dynamic model of a parafoil is complex and nonlinear, so that the problem can only be solved numerically. However, in what follows we will make some assumptions, allowing an analytical solution to be used as a reference trajectory in the control algorithm. These assumptions are: a) the turn rate is slow, so that the roll and sideslip angles can be ignored, and b) the descent rate V_v^* and air speed V_h^* are viewed as nearly constant (defined by the canopy, lines, etc. and treated as the known values). In this case it immediately follows that

$$t_2 = t_{start} - \frac{z_{start}}{V_v^*}. \tag{1}$$

The problem reduces to handling a simple kinematic model represented by three components of the ground velocity as:

$$\begin{bmatrix} \dot{x} \\ \dot{y} \\ \dot{z} \end{bmatrix} = \begin{bmatrix} -W + V_h^* \cos\psi \\ V_h^* \sin\psi \\ V_v^* \end{bmatrix}. \tag{2}$$

Now, the reference turn function $\psi(t)$ can be chosen as any function that satisfies the boundary conditions $\psi(t_0) = 0$ and $\psi(t_1) = -\pi$ (for the left pattern as shown on Fig. B). For instance, for a linear turn (constant turn rate) the solution to the required turn rate and the final turn time T_{turn} are provided by:

$$\dot{\psi} = -\frac{V_h^*}{R} \quad \text{and} \quad T_{turn} = \frac{\pi R}{V_h^*}. \tag{3}$$

Hence, the most straightforward algorithm to control the descending system at the terminal phase is to control its turn rate for example as follows:

$$\dot{\psi}^c = \mp \frac{V_h^*}{R} \tag{4}$$

(the plus-minus signs correspond to the left and right turn, respectively). After the final turn the system travels directly to the desired target. Assuming that the wind W is constant all way down and a constant turn rate (3), integration of inertial velocities along axes *x* and *y* from t_{start} to t_2 (Phases 4-6) yields two simple equalities:

$$D_{switch} - \int_{t_0}^{t_1} \dot{x}dt - \int_{t_1}^{t_2} \dot{x}dt = D_{switch} - WT_{turn} - (V_h^* + W)T_{app} = 0, \tag{5}$$

$$z + V_v^* \left(\frac{L + D_{switch}}{V_h^* - W} \right) + V_v^* t_{turn} + V_v^* t_{app} = 0 . \quad (6)$$

Resolving them with respect to D_{switch} and a T_{app} results in

$$D_{switch} = WT_{turn} + \left(\frac{V_h^{*2} - W^2}{2V_h^*} \right) \left(\frac{-z}{V_v^*} - T_{turn} - \frac{L + WT_{turn}}{V_h^* - W} \right), \quad (7)$$

$$T_{app} = \left(\frac{V_h^* - W}{2V_h^*} \right) \left(\frac{-z}{V_v^*} - T_{turn} \right) - \frac{L + WT_{turn}}{2V_h^*} . \quad (8)$$

From Eqs.(7) and (8) it can be seen that the higher the altitude z, the larger D_{switch} and T_{app} become. As the parafoil loiters upwind of the target, z_{start} the altitude at which to turn towards the target can be found by using a desired final approach time T_{app}^{des}. The switching altitude to achieve T_{app}^{des} is then given by solving Eq.(8) for z leading to the following expression:

$$z_{start} = -V_v^* \left(T_{turn} + \frac{L + WT_{turn}}{V_h^* - W} + \frac{2V_h^*}{V_h^* - W} T_{app}^{des} \right) = V_v^* \frac{L + V_h^* (T_{turn} + 2T_{app}^{des})}{W - V_h^*} . \quad (9)$$

Once the system is traveling towards the target the goal is to bring the system from its initial state at the top of the downwind led to the point defined by $x_T = D_{switch}$ and $y_T = \mp 2R$ (for the left and right turn, respectively). The distance $\hat{D}_{switch}$ is estimated during the downwind leg constantly using the analogue of Eq.(7):

$$\hat{D}_{switch} = \hat{W} T_{turn} + \left(\frac{\hat{V}_h^{*2} - \hat{W}^2}{2\hat{V}_h^*} \right) \left(\frac{-\hat{z}}{\hat{V}_v^*} - T_{turn} - \frac{\hat{x} + \hat{W} T_{turn}}{\hat{V}_h^* - \hat{W}} \right) = - \frac{\hat{z}(\hat{V}_h^{*2} - \hat{W}^2) + \hat{V}_h^* \hat{V}_v^* T_{turn} (\hat{V}_h^* - \hat{W}) + \hat{x} \hat{V}_v^* (\hat{V}_h^* + \hat{W})}{2\hat{V}_h^* \hat{V}_v^*} , \quad (10)$$

where $\hat{V}_h^*$, $\hat{V}_v^*$ and $\hat{W}$ are the estimates of the corresponding parameters at current position $(\hat{x}, \hat{z})$. Note, Eq.(10) produces the value of $\hat{D}_{switch}$ in the assumption that V_h^*, V_v^* and W remain constant from the current altitude all way down.

[0102] Appendix C

Optimal Terminal Guidance

To overcome the difficulties of fighting unaccounted winds the following two-point boundary-value problem (TPBVP) was formulated. Staring at some initial point at $t=0$ with the state vector defined as $\mathbf{x}_0=\left[x_0,y_0,\psi_0\right]^T$ we need to bring our ADS influenced by the last known constant wind $\mathbf{w}=\left[W,0,0\right]^T$ to another point, $\mathbf{x}_f=\left[\left(V_h^*+W\right)T_{app}^{des},0,-\pi\right]^T$ (for consistency with Appendix B we will consider a left pattern turn) at $t=t_f$. Hence, we need to find the trajectory that satisfies these boundary conditions along with a constraint imposed on control (yaw rate), $|\dot{\psi}|\le\dot{\psi}_{\max}$, while finishing the maneuver in exactly T_{turn} seconds (if needed, the performance index may also include additional terms related to the compactness of the maneuver and/or control expenditure). The found optimal control $\dot{\psi}_{opt}(t)$ is then tracked by the ADS GNC unit using the MPC algorithm in Appendix A. Unaccounted winds $\mathbf{w}^{dist}=\left[w_x,w_y,0\right]^T$ (the vertical component will be accounted for indirectly via estimating the current $\hat{V}_v$) will not allow exact tracking of the calculated optimal trajectory. Computation of the optimal trajectory will be updated during the final turn, each time starting from the current (off the original trajectory) initial conditions, requiring the ADS to be at $\mathbf{x}_f=\left[\left(V_h^*+W\right)T_{app}^{des},0,-\pi\right]^T$ in T_{turn} seconds from the beginning of the turn. The remaining time until arrival at the final approach is computed as

$$t_f=-\frac{\hat{z}}{\hat{V}_v}-T_{app}^{final}, \tag{1}$$

where T_{app}^{final} is the final calculated approach time from Eq.(8) before entering the final turn.

Development of the optimal trajectory algorithm begins by recalling from Eq.(2) the horizontal trajectory knimematics:

$$\begin{bmatrix}\dot{x}\\ \dot{y}\end{bmatrix}=\begin{bmatrix}-W+V_h^*\cos\psi\\ V_h^*\sin\psi\end{bmatrix}. \tag{2}$$

Recognizing that if the final turn horizontal trajectory is given by Eq.(2) the yaw angle along this trajectory is related to the change of inertial coordinates as follows:

$$\psi=\tan^{-1}\frac{\dot{y}}{\dot{x}+W}. \tag{3}$$

Differentiating (3) provides the yaw rate control required to follow the reference final turn trajectory in presence of constant wind *W*:

$$\dot{\psi}=\frac{\ddot{y}(\dot{x}+W)-\ddot{x}\dot{y}}{(\dot{x}+W)^2+\dot{y}^2}. \tag{4}$$

The inertial (ground) speed along the trajectory will also depend on the current yaw angle:

$$|V_G| = \sqrt{\dot{x}^2 + \dot{y}^2} = \sqrt{V_h^{*2} + W^2 - 2V_h^* W \cos\psi}\ . \tag{5}$$

Now, following the general idea of direct methods of calculus of variations (e.g., see Yakimenko, O., "Direct Method for Rapid Prototyping of Near-Optimal Aircraft Trajectories," AIAA Journal of Guidance, Control, and Dynamics, vol.23, no.5, 2000, pp.865-875.) we will assume the solution of the TPBVP to be represented analytically as functions of some scaled abstract argument $\bar{\tau} = \tau / \tau_f \in [0;1]$:

$$\begin{aligned} x(\bar{\tau}) &= P_1(\bar{\tau}) = a_0^1 + a_1^1\bar{\tau} + a_2^1\bar{\tau}^2 + a_3^1\bar{\tau}^3 + b_1^1 \sin(\pi\bar{\tau}) + b_2^1 \sin(2\pi\bar{\tau}), \\ y(\bar{\tau}) &= P_2(\bar{\tau}) = a_0^2 + a_1^2\bar{\tau} + a_2^2\bar{\tau}^2 + a_3^2\bar{\tau}^3 + b_1^2 \sin(\pi\bar{\tau}) + b_2^2 \sin(2\pi\bar{\tau}). \end{aligned} \tag{6}$$

The coefficients a_i^η and b_i^η ($\eta = 1,2$) in these formulas are defined by the boundary conditions up to the second-order derivative at $\tau = 0$ and $\tau = \tau_f$ ($\bar{\tau} = 1$). According to the problem formulation and Eq.(2) these boundary conditions are as follows:

$$\begin{bmatrix} x \\ y \end{bmatrix}_{\tau=0} = \begin{bmatrix} x_0 \\ y_0 \end{bmatrix}, \begin{bmatrix} \dot{x} \\ \dot{y} \end{bmatrix}_{\tau=0} = \begin{bmatrix} -W + V_h^* \cos\psi_0 \\ V_h^* \sin\psi_0 \end{bmatrix}, \begin{bmatrix} \ddot{x} \\ \ddot{y} \end{bmatrix}_{\tau=0} = \begin{bmatrix} -\dot{\psi}_0 V_h^* \sin\psi_0 \\ \dot{\psi}_0 V_h^* \cos\psi_0 \end{bmatrix}, \tag{7}$$

$$\begin{bmatrix} x \\ y \end{bmatrix}_{\tau=\tau_f} = \begin{bmatrix} \left(V_h^* + W\right) T_{app}^{des} \\ 0 \end{bmatrix}, \begin{bmatrix} \dot{x} \\ \dot{y} \end{bmatrix}_{\tau=\tau_f} = \begin{bmatrix} -W - V_h^* \\ 0 \end{bmatrix}, \begin{bmatrix} \ddot{x} \\ \ddot{y} \end{bmatrix}_{\tau=\tau_f} = \begin{bmatrix} 0 \\ 0 \end{bmatrix}. \tag{8}$$

While the final conditions (8) will be constant (the second derivatives are zeroed for a smooth arrival), the initial conditions will reflect the current state of the system at each cycle of optimization. Let us now differentiate Eqs.(6) two times with respect to τ to get:

$$\begin{aligned} \tau_f P_\eta'(\bar{\tau}) &= a_1^\eta + 2a_2^\eta\bar{\tau} + 3a_3^\eta\bar{\tau}^2 + \pi b_1^\eta \cos(\pi\bar{\tau}) + 2\pi b_2^\eta \cos(2\pi\bar{\tau}), \\ \tau_f^2 P_\eta''(\bar{\tau}) &= 2a_2^\eta + 6a_3^\eta\bar{\tau} - \pi^2 b_1^\eta \sin(\pi\bar{\tau}) - (2\pi)^2 b_2^\eta \sin(2\pi\bar{\tau}). \end{aligned} \tag{9}$$

Equating these derivatives at the terminal points to the known boundary conditions (7)-(8) yields a system of linear algebraic equations to solve for coefficients a_i^η and b_i^η ($\eta = 1,2$). For instance, for the *x*-coordinate we'll get

$$\begin{bmatrix} 1 & 0 & 0 & 0 & 0 & 0 \\ 1 & 1 & 1 & 1 & 0 & 0 \\ 0 & 1 & 0 & 0 & \pi & 2\pi \\ 0 & 1 & 2 & 3 & -\pi & 2\pi \\ 0 & 0 & 2 & 0 & 0 & 0 \\ 0 & 0 & 2 & 6 & 0 & 0 \end{bmatrix} \begin{bmatrix} a_0^1 \\ a_1^1 \\ a_2^1 \\ a_3^1 \\ b_1^1 \\ b_2^1 \end{bmatrix} = \begin{bmatrix} x_0 \\ x_f \\ x_0'\tau_f \\ x_f'\tau_f \\ x_0''\tau_f^2 \\ x_f''\tau_f^2 \end{bmatrix} \tag{10}$$

Being resolved this system yields

$$a_0^1 = x_0,\quad a_1^1 = -(x_0 - x_f) + \frac{(2x_0'' + x_f'')\tau_f^2}{6},\quad a_2^1 = \frac{x_0''\tau_f^2}{2},\quad a_3^1 = -\frac{(x_0'' - x_f'')\tau_f^2}{6};$$
$$b_1^1 = \frac{2(x_0' - x_f')\tau_f + (x_0'' + x_f'')\tau_f^2}{4\pi},\quad b_2^1 = \frac{12(x_0 - x_f) + 6(x_0' + x_f')\tau_f + (x_0'' - x_f'')\tau_f^2}{24\pi}. \tag{11}$$

The only problem is that the derivatives in Eqs.(11) are taken in the virtual domain, while the actual boundary conditions are given in the physical domain. Mapping between the virtual domain $[0;\tau_f]$ and physical domain $[0;t_f]$ is addressed by introducing a speed factor λ:

$$\lambda = \frac{d\tau}{dt}, \tag{12}$$

Using this speed factor we may now compute corresponding derivatives in the virtual domain using the obvious differentiation rules valid for any time-variant parameter ξ:

$$\dot{\xi} = \lambda\xi',\ \ddot{\xi} = \lambda\left(\lambda'\xi' + \lambda\xi''\right). \tag{13}$$

Inverting Eqs.(13) yield:

$$\xi' = \lambda^{-1}\dot{\xi},\ \xi'' = \lambda^{-2}\ddot{\xi} - \lambda'\lambda^{-1}\dot{\xi}. \tag{14}$$

Note that we only need to use Eqs.(14) once to transfer the boundary conditions. Since the speed factor λ simply scales the entire problem – the higher speed factor λ is, the larger τ_f it results in (see explanation in Lukacs, J., and Yakimenko, O., "Trajectory-Shaping Guidance for Interception of Ballistic Missiles during the Boost Phase," AIAA Journal of Guidance, Control, and Dynamics, vol.31, no.5, 2008, pp.1524-1531.) – we may let

$$\lambda_{0;f} = 1 \text{ and } \lambda'_{0;f} = 0, \tag{15}$$

which means we can safely assume

$$\xi' = \dot{\xi},\ \xi'' = \ddot{\xi}. \tag{16}$$

Now let us describe the numerical procedure for finding the optimal solution among all candidate trajectories described by Eqs.(6). First, we guess the value of the only varied parameter τ_f and compute the coefficients of the candidate trajectory using Eqs.(11) with the boundary conditions (7) and (8) converted to the virtual domain via Eqs.(14) (accounting for Eqs.(15)). For the initial value of τ_f we can take the length of the circumference connecting terminal points:

$$\tau_f = \frac{\pi}{2}\sqrt{(x_f - x_0)^2 + (y_f - y_0)^2}. \tag{17}$$

Having an analytical representation of the candidate trajectory, Eqs.(6) and (9), define the values of x_j, y_j, x_j', and y_j', $j = 1,\ldots,N$ over a fixed set of N points spaced evenly along the virtual arc $[0;\tau_f]$ with the interval

$$\Delta\tau = \tau_f(N-1)^{-1}, \tag{18}$$

so that

$$\tau_j = \tau_{j-1} + \Delta\tau\,,\ \ j = 2,\ldots,N\,,\ (\tau_1 = 0)\,. \tag{19}$$

Then, for each node $j = 2,\ldots,N$ we compute

$$\Delta t_{j-1} = \frac{\sqrt{(x_j - x_{j-1})^2 + (y_j - y_{j-1})^2}}{\sqrt{V_h^{*2} + W^2 - 2V_h^* W\cos\psi_{j-1}}} \tag{20}$$

($\psi_1 \equiv \psi_0$), and

$$\lambda_j = \Delta\tau\Delta t_{j-1}^{-1}\,. \tag{21}$$

The yaw angle ψ can now be computed using the virtual domain version of Eq.(3):

$$\psi_j = \tan^{-1}\frac{\lambda_j y_j'}{\lambda_j x_j' + W}\,. \tag{22}$$

Finally, the yaw rate $\dot{\psi}$ is evaluated using Eq.(4) (with time derivatives evaluated using Eq.(23)) or simply as

$$\dot{\psi}_j = (\psi_j - \psi_{j-1})\Delta t_{j-1}^{-1}\,. \tag{23}$$

When all parameters (states and controls) are computed in each of the *N* points, we can compute the performance index

$$J = \left(\sum_{j=1}^{N-1}\Delta t_j - T_{turn}\right)^2 + k^{\dot{\psi}}\Delta\,, \tag{24}$$

where

$$\Delta = \max_j\left(0;\left|\dot{\psi}_j\right| - \dot{\psi}_{\max}\right)^2 \tag{25}$$

with $k^{\dot{\psi}}$ being a scaling (weighting) coefficient. Now the problem can be solved say in the Mathworks' development environment with as simple built-in optimization function as *fminbnd*. It should be noted that the numerical algorithm based on the direct method introduced in this Appendix with the non-gradient optimization routine *fminbnd* based on the straight forward golden section search and parabolic interpolation algorithm allows computing the optimal turn trajectory very fast. To be more specific a 16bit 80MHz processor, allowed computation of the 17.5 second turn maneuver with *N* = 20 in 10 iterations, which took only 0.07s all together. With the controls update rate of 0.25s that means that the trajectory can be updated as often as every control cycle.

[0103] Appendix D

More General Optimal Terminal Guidance with Known Wind Profiles

The optimal turn computation presented in Appendix C for the simple case of a constant speed profile can be generalized even further if there is more information about the winds known a priori. For example, assume that instead of a constant x-component of the prevailing wind versus altitude *h* we have a linear profile

$$W(h) = W_G + kh \tag{1}$$

where W_G is a known ground wind and coefficient $k = \frac{W_0 - W_G}{h_0}$ is defined by the ground wind W_G and wind W_0 measured at altitude $h_0 = -z_0$ (corresponding to the point where the final turn begins).

Then, the two-point boundary-value problem will be formulated for a slightly different system of kinematic equations

$$\begin{bmatrix} \dot{x} \\ \dot{y} \end{bmatrix} = \begin{bmatrix} -W(h) + V_h^* \cos\psi \\ V_h^* \sin\psi \end{bmatrix} \tag{2}$$

and different boundary conditions. To be more specific, staring from some different initial point, defined by a different expression for a D_{switch}, we will need to bring a parafoil to the point

$$\mathbf{x}_f = \left[\left(V_h^* + W \right) T_{app}^{des} + \frac{k}{2} V_v^* (T_{app}^{des})^2, 0, -\pi \right]^T \tag{8}$$

To compute the offset in Eq.(8) we used the fact that the final approach starts at the altitude $V_v^* T_{app}^{des}$, so that using the obvious relation

$$dt = \frac{dh}{V_v^*} \tag{9}$$

we may write

$$x_f = \int_0^{T_{app}^{des}} \left(V_h^* + W \right) dt = \int_0^{V_v^* T_{app}^{des}} \left(V_h^* + W \right) \frac{dh}{V_v^*} = \left(V_h^* + W_G \right) T_{app}^{des} + \frac{k}{2} V_v^* (T_{app}^{des})^2 \tag{10}$$

In this case, inverting equations (7) yeilds

$$\psi = \tan^{-1} \frac{\dot{y}}{\dot{x} + W(h)} \tag{11}$$

and its differentiation should account for Eq.(6), so that

$$\dot{\psi} = \frac{\ddot{y}(\dot{x}+W)-(\ddot{x}+\dot{W})\dot{y}}{(\dot{x}+W)^2+\dot{y}^2} = \frac{\ddot{y}(\dot{x}+W)-(\ddot{x}+kV_v^*)\dot{y}}{(\dot{x}+W)^2+\dot{y}^2}. \quad (12)$$

The only modifications the numerical algorithm will require is that it will involve the new boundary conditions

$$\begin{bmatrix}\dot{x}\\ \dot{y}\end{bmatrix}_{\tau=0} = \begin{bmatrix}-W_0+V_h^*\cos\psi_0\\ V_h^*\sin\psi_0\end{bmatrix}, \quad \begin{bmatrix}\ddot{x}\\ \ddot{y}\end{bmatrix}_{\tau=0} = \begin{bmatrix}-kV_v^*-\dot{\psi}_0V_h^*\sin\psi_0\\ \dot{\psi}_0V_h^*\cos\psi_0\end{bmatrix}, \quad (13)$$

$$\begin{bmatrix}x\\ y\end{bmatrix}_{\tau=\tau_f} = \begin{bmatrix}\left(V_h^*+W_G\right)T_{app}^{des}+\frac{k}{2}V_v^*(T_{app}^{des})^2\\ 0\end{bmatrix}, \quad \begin{bmatrix}\dot{x}\\ \dot{y}\end{bmatrix}_{\tau=\tau_f} = \begin{bmatrix}-W_G-kV_v^*T_{app}^{des}-V_h^*\\ 0\end{bmatrix}, \quad (14)$$

computation of an altitude

$$h_j = h_{j-1}-V_v^*\Delta t_{j-1},\ j=2,\ldots,N,\ (h_1=-z_0). \quad (15)$$

and the corresponding wind magnitude

$$W_j = W_G+kh_j \quad (16)$$

The latter two values will be used in

$$\Delta t_{j-1} = \sqrt{\frac{(x_j-x_{j-1})^2+(y_j-y_{j-1})^2}{V_h^{*2}+0.25(W_j+W_{j-1})^2-V_h^*(W_j+W_{j-1})\cos\psi_{j-1}}} \quad (17)$$

and

$$\psi_j = \tan^{-1}\frac{\lambda_j y_j'}{\lambda_j x_j'+W_j}. \quad (18)$$

In the case of a logarithmic wind profile

$$W(h) = \beta+a\ln(h) \quad (19)$$

some of the above equations will be replaced with the new ones

$$x_f = \int_0^{V_v^*T_{app}^{des}}\left(V_h^*+W\right)\frac{dh}{V_v^*} = \left(V_h^*+\alpha-\beta\right)T_{app}^{des}+\beta T_{app}^{des}\ln(V_v^*T_{app}^{des}) \quad (20)$$

$$\begin{bmatrix}\ddot{x}\\ \ddot{y}\end{bmatrix}_{\tau=0} = \begin{bmatrix}-ah_0^{-1}V_v^*-\dot{\psi}_0V_h^*\sin\psi_0\\ \dot{\psi}_0V_h^*\cos\psi_0\end{bmatrix}, \quad (21)$$

$$\begin{bmatrix}x\\ y\end{bmatrix}_{\tau=\tau_f} = \begin{bmatrix}\left(V_h^*+\alpha-\beta\right)T_{app}^{des}+\beta T_{app}^{des}\ln(V_v^*T_{app}^{des})\\ 0\end{bmatrix}, \quad \begin{bmatrix}\dot{x}\\ \dot{y}\end{bmatrix}_{\tau=\tau_f} = \begin{bmatrix}-\beta-a\ln(V_v^*T_{app}^{des})-V_h^*\\ 0\end{bmatrix}, \quad (22)$$

and

$$W_j = \beta + a\ln(h_j) \tag{23}$$

The remaining ones will be the same.

Similarly, the optimization routine can accommodate crosswinds is they are known in one form or another. This may happen when the horizontal winds profile versus altitude is available. Consider

$$W_x(h) = f_x(h), \quad W_y(h) = f_y(h) \tag{24}$$

to be x- and y- components of a horizontal wind profile approximated with some analytical dependence (e.g. of the form of Eq.(6) or (16) or cubic spline). Then, we can write

$$\begin{bmatrix} \dot{x} \\ \dot{y} \end{bmatrix} = \begin{bmatrix} -W_x(h) + V_h^* \cos\psi \\ W_y(h) + V_h^* \sin\psi \end{bmatrix} \tag{25}$$

The final point will then be defined as

$$\mathbf{x}_f = \left[x_f, y_f, -\pi\right]^T \tag{26}$$

where offsets in x- and y- directions will be computed as

$$x_f = V_h^* T_{app}^{des} + \int_0^{V_v^* T_{app}^{des}} W_x(h)\frac{dh}{V_v^*}, \quad y_f = -\int_0^{V_v^* T_{app}^{des}} W_y(h)\frac{dh}{V_v^*} \tag{27}$$

The heading angle equation will look as

$$\psi = \tan^{-1}\frac{\dot{y} - W_y(h)}{\dot{x} + W_x(h)} \tag{28}$$

while its derivative will be presented by

$$\dot{\psi} = \frac{(\ddot{y} - W_y'(h)V_v^*)(\dot{x} + W_x(h)) - (\ddot{x} + W_x'(h)V_v^*)(\dot{y} - W_y(h))}{(\dot{x} + W_x(h))^2 + (\dot{y} - W_y(h))^2} \tag{29}$$

The total speed will be expressed as

$$|V_G| = \sqrt{\dot{x}^2 + \dot{y}^2} = \sqrt{V_h^{*2} + \left(W_x(h) + W_y(h)\right)^2 - 2V_h^*\left(W_x(h)\cos\psi - W_y(h)\sin\psi\right)}. \tag{30}$$

The numerical procedure will proceed with the boundary conditions

$$\begin{bmatrix} x \\ y \end{bmatrix}_{\tau=0} = \begin{bmatrix} x_0 \\ y_0 \end{bmatrix}, \quad \begin{bmatrix} \dot{x} \\ \dot{y} \end{bmatrix}_{\tau=0} = \begin{bmatrix} -W_x(h_0) + V_h^*\cos\psi_0 \\ W_y(h_0) + V_h^*\sin\psi_0 \end{bmatrix}, \quad \begin{bmatrix} \ddot{x} \\ \ddot{y} \end{bmatrix}_{\tau=0} = \begin{bmatrix} -W_x'(h)V_y^* - \dot{\psi}_0 V_h^*\sin\psi_0 \\ W_y'(h)V_y^* + \dot{\psi}_0 V_h^*\cos\psi_0 \end{bmatrix}, \tag{31}$$

$$\begin{bmatrix} x \\ y \end{bmatrix}_{\tau=\tau_f} = \begin{bmatrix} x_f \\ y_f \end{bmatrix}, \quad \begin{bmatrix} \dot{x} \\ \dot{y} \end{bmatrix}_{\tau=\tau_f} = \begin{bmatrix} -W_x(h) - V_h^* \\ W_y(h) \end{bmatrix}, \quad \begin{bmatrix} \ddot{x} \\ \ddot{y} \end{bmatrix}_{\tau=\tau_f} = \begin{bmatrix} 0 \\ 0 \end{bmatrix}. \tag{32}$$

and will involve computing wind components at each step

$$W_{xj} = f_x(h_j) \quad \text{and} \quad W_{yj} = f_y(h_j) \tag{33}$$

to be used in the numerical equations similar to those above.

[0104] Appendix E

Ballistic Winds

For operational use the vertical winds profile can be reduced to the so-called ballistic winds. In other words, if at some altitude H we have a ballistic wind of magnitude W_B and direction Ψ_W, then the effect of variable winds $w(h)$ for some system with the descent rate V_v on its way from altitude H down to the surface is reduced to simple formulas:

$$\begin{aligned} x(h) &= \frac{H}{V_v} W_B \cos\Psi_W \\ y(h) &= \frac{H}{V_v} W_B \sin\Psi_W \end{aligned} \tag{1}$$

or in other words

$$\begin{aligned} \int_0^H \frac{1}{V_v} w(h)\cos\psi_w(h)dh &= \frac{H}{V_v} W_B \cos\Psi_W \\ \int_0^H \frac{1}{V_v} w(h)\sin\psi_w(h)dh &= \frac{H}{V_v} W_B \sin\Psi_W \end{aligned} \tag{2}$$

Substituting integrals with the finite sum of trapezoids based on the discrete values of h_k, w_k and $\psi_{w;k}$, $k = 1,\ldots,M$, we get

$$\begin{aligned} \sum_{k=2}^{M}(h_k - h_{k-1})\frac{w_k\cos\psi_{w;k} + w_{k-1}\cos\psi_{w;k-1}}{2} &= h_M W_M \cos\Psi_{W;M} \\ \sum_{k=2}^{M}(h_k - h_{k-1})\frac{w_k\sin\psi_{w;k} + w_{k-1}\sin\psi_{w;k-1}}{2} &= h_M W_M \sin\Psi_{W;M} \end{aligned} \tag{3}$$

The index starts from 2 because by definition the winds measurements at the lowest altitude can be considered ballistic winds at this altitude.

From Eqs.(3) it further follows that

$$\begin{aligned} \tan\Psi_{W;M} &= \frac{\sum_{k=2}^{M}(h_k - h_{k-1})(w_k\sin\psi_{w;k} + w_{k-1}\sin\psi_{w;k-1})}{\sum_{k=2}^{M}(h_k - h_{k-1})(w_k\cos\psi_{w;k} + w_{k-1}\cos\psi_{w;k-1})} \\ W_M &= \frac{1}{2h_M}\sqrt{\left(\sum_{k=2}^{M}(h_k - h_{k-1})(w_k\cos\psi_{w;k} + w_{k-1}\cos\psi_{w;k-1})\right)^2 + \left(\sum_{k=2}^{M}(h_k - h_{k-1})(w_k\sin\psi_{w;k} + w_{k-1}\sin\psi_{w;k-1})\right)^2} \end{aligned} \tag{4}$$

For the specific case when $h_k - h_{k-1} = \Delta h = const$, $k = 2,\ldots,M$, Eqs.(42) can be further reduced to

$$\tan \Psi_{W,M} = \frac{\sum_{k=2}^{M} \left(w_k \sin \psi_{w;k} + w_{k-1} \sin \psi_{w;k-1} \right)}{\sum_{k=2}^{M} \left(w_k \cos \psi_{w;k} + w_{k-1} \cos \psi_{w;k-1} \right)} \tag{5}$$

$$W_M = \frac{\Delta h}{2 h_M} \sqrt{\left(\sum_{k=2}^{M} \left(w_k \cos \psi_{w;k} + w_{k-1} \cos \psi_{w;k-1} \right) \right)^2 + \left(\sum_{k=2}^{M} \left(w_k \sin \psi_{w;k} + w_{k-1} \sin \psi_{w;k-1} \right) \right)^2}$$

[0105] Appendix F

Logarithmic Winds Model

In the following derivation, the assumption of a constant or piecewise constant wind profile will be discarded and replaced by the assumption that wind speed *W* varies logarithmically with altitude *z* as:

$$W(h) = (m_W)\ln(h/h_0), \quad (W(h) = 0, \text{ for } h \le h_0) \tag{1}$$

where α and β are constants. Note that, since altitude *z* is represented as a negative number according to the sign convention in use, an additional factor of −1 is included in the argument of the logarithm. The derivation uses this assumption for the wind profile, along with the assumptions that the steady-state, no-wind values of the ADS horizontal and vertical velocities are known and labeled V_h^* and V_v^*. Furthermore, it is assumed that the wind vector lies only in the horizontal plane, and is parallel with the *x* axis of the coordinate system depicted in Fig. B in Appendix B. Using the assumptions of constant steady-state no-wind vertical velocity and no vertical wind component, the time derivative of the z coordinate, ˙z, is just equal to V_v^*, where downward change has a positive sign. Thus, the z-budget equation in Appendix B can be simplified.

$$z_{\text{start}} + V_v^* T_{\text{downwind}} + V_v^* T_{\text{turn}} + V_v^* T_{\text{app}} = 0 \tag{2}$$

where $T_{downwind}$ represents the time duration required to travel the sum of distances L and D_{switch}. Again, recall that under the sign convention being used here, zstart is a negative number and that V_v^* and all time durations are positive. Assuming that the Snowflake's turn rate is constant, and that the turn will encompass 180° of a circle of known radius R, the time duration for the turn T_{turn} is a known constant in terms of R and V_h^* (see Appendix B, Eq. 33). Therefore, this equation has only two unknowns: $T_{downwind}$ and T_{app}.

Under the assumption of a constant wind profile, a simple expression for $T_{downwind}$ could be written in terms of unknown value D_{switch}. Also using the constant wind profile assumption, the *x*-budget equation in Appendix B can be simplified into an equation containing two unknowns: D_{switch} and T_{app}; therefore the two linear equations in two unknowns could easily be solved. Under the assumption of a logarithmic wind profile as in Eq. (1) on the current page, $T_{downwind}$ cannot be replaced by a simple expression containing D_{switch}. Instead, in order to compute $T_{downwind}$ assuming that the wind profile is logarithmic, a value of D_{switch} must be assumed, and then the time t0 can be computed. Time t0 is computed using the assumption of constant vertical velocity from the following simple relation:

$$t_0 = \frac{z_0 - z_{\text{start}}}{V_v^*} + t_{\text{start}} \tag{3}$$

where altitude z0 had been calculated using the Lambert *W* function as follows:

$$z_0 = \frac{c}{bW\left(-\frac{ce^{a/b}}{b}\right)} \tag{4}$$

where *a*, *b*, and *c* are constants that can be expressed in terms of known quantities V_h^*, V_v^*, a, b, *L*, z_{start}, and assumed quantity D_{switch}.

The iteration procedure to calculate D_{switch} is as follows:

1. Select an initial guess value for D_{switch}
2. Using the initial guess value for Dswitch, calculate z_0 using Eq. (4) on this page, and T_{downwind} from:

$$T_{\text{downwind}} = \frac{z_0 - z_{\text{start}}}{V_v^*} \tag{5}$$

3. Using T_{downwind}, calculate T_{app} using Eq. (2) on the previous page

$$T_{\text{app}} = \frac{-z_{\text{start}}}{V_v^*} - T_{\text{turn}} - T_{\text{downwind}} \tag{6}$$

4. Compute z_1 using the assumption of constant vertical velocity

$$z_1 = z_0 + V_v^* T_{\text{turn}} \tag{7}$$

5. Compute ~D from known quantities:

$$\tilde{D} = \left(-m_W \ln(h_0) - m_W\right) T_{\text{turn}} - \frac{m_W}{V_v^*}\left[-z_0 \ln\left(-z_0\right) - z_1 \ln\left(-z_1\right)\right] \tag{8}$$

6. Compute L_{app} using T_{app} using:

$$L_{\text{app}} = \left(V_h^* - m_W \ln(h_0) - m_W\right) T_{\text{app}} + \frac{m_W h_0}{V_v^*} + m_W T_{\text{app}} \ln\left(T_{\text{app}} V_v^*\right) \tag{9}$$

7. Compute D_{switch} from:

$$D_{\text{switch}} = \tilde{D} + L_{\text{app}} \tag{10}$$

8. Use value of D_{switch} computed in step 7 as the next iteration estimate of D_{switch} in step 1. Repeat iterations until differences between subsequent values of D_{switch} are below a threshold value.

1. A method comprising:

establishing a wireless network between a wireless access node of an existing network and a remote location by wirelessly linking a plurality of electronic processing circuits each transported by a respective parafoil, said wirelessly linked processing circuits to route packets from said wireless access node to said remote location.

2. The method of claim **1** wherein said wireless network is established while said parafoils are descending.

3. The method of claim **2** further comprising causing said wireless network to be no longer operative before said parafoils land.

4. The method of claim **1** further comprising sending notice to said remote location that communication to said remote location is desired.

5. The method of claim **1** further comprising configuring routing tables of said electronic processing circuits.

6. An apparatus, comprising:

a first parafoil's payload assembly having first electronic circuitry to establish a wireless link with second electronic circuitry of a second parafoil's payload assembly, said first electronic circuitry including routing information to route a packet from said first parafoil's payload assembly to said second parafoil's payload assembly over said wireless link, said packet wirelessly received at said first parafoil's payload assembly beforehand.

7. The apparatus of claim **6** wherein said first electronic circuitry is part of an electronic control unit of said first parafoil that automatically controls said first parafoil's flight path during said first parafoil's descent.

8. The apparatus of claim **7** wherein said wireless link is to be established while said first parafoil and said second parafoil are descending.

9. The apparatus of claim **8** wherein said wireless link is to be extinguished before said first parafoil lands.

10. The apparatus of claim **7** wherein said first electronic circuitry is also to establish a second wireless link with third electronic circuitry of a third parafoil's payload assembly, said first electronic circuitry including routing information to route a second packet from said first parafoil's payload assembly to said third parafoil's payload assembly over said second wireless link, said second packet wirelessly received at said first parafoil's payload assembly beforehand, said second packet sent from said second electronic circuitry of said second parafoil payload assembly, beforehand.

11. The apparatus of claim **10** wherein said second wireless link is to be established while said first parafoil and said second parafoil are descending.

12. The apparatus of claim **11** wherein said second wireless link is to be extinguished before said first parafoil lands.

13. The apparatus of claim **6** wherein said first electronic circuitry is also to establish a second wireless link with third electronic circuitry of a third parafoil's payload assembly, said first electronic circuitry including routing information to route a second packet from said first parafoil's payload assembly to said third parafoil's payload assembly over said second wireless link, said second packet wirelessly received at said first parafoil's payload assembly beforehand, said second packet sent from said second electronic circuitry of said second parafoil payload assembly, beforehand.

* * * * *